

Home Control and Monitoring System using MATLAB Graphical User Interface

Thae Hsu Thoung⁽¹⁾, Dr. Zin Ma Ma Myo⁽²⁾

⁽¹⁾Technological University (Taunggyi), Myanmar

⁽²⁾ Technological University (Banmaw), Myanmar

Email: thaehsuthoungmtuec@gmail.com

ABSTRACT: This paper describes the home control and monitoring system using MATLAB Graphical User Interface (GUI). The system consists of twelve GUI controls to switch on or off electric devices such as light, air conditioner, fan, air cooler, printer, water pump, garden sprinkler, etc. It also includes temperature and humidity monitoring to get weather information. The system consists of human detection for home security. Water level detection is also included to alert the user whether the water tank is full or not. It will provide ease of use with the capability of controlling and monitoring home environment via personal computer.

KEYWORDS: MATLAB, GUI controls, temperature, human detection, water level

1. INTRODUCTION

Traditionally home appliances are controlled via switches so that the user is needed to go near them to control and operate. This paper focuses on effective system that can be controlled and monitored home environment via personal computer.

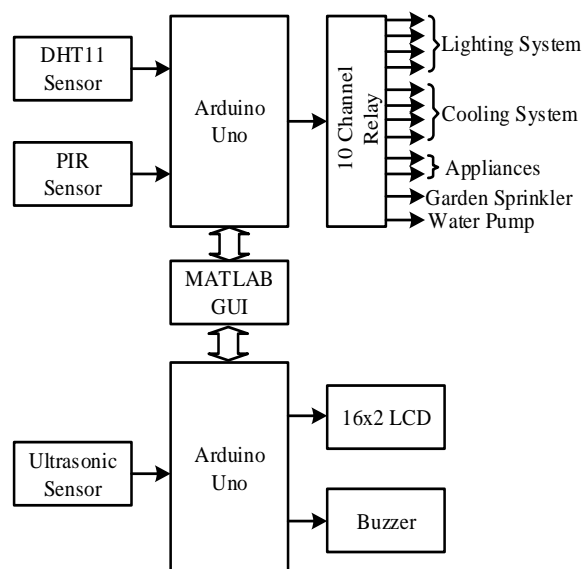


Fig 1 Block Diagram of Home Control and Monitoring System

Fig 1 shows the block diagram of home control and monitoring system. DHT11 sensor detects the temperature and humidity levels in the home. This real time weather information will be displayed on MATLAB GUI via Arduino UNO.

For home security, PIR sensor is used to detect human movement. When the movement is detected, human detection message “Movement Detected” will be shown in MATLAB GUI. If there is no movement, “No Movement” message will be displayed on MATLAB GUI.

The ultrasonic sensor is used to detect water level in the tank. If the water tank is full of water, red LED will be lighted on and the buzzer will give alert to user to switch off the water pump. To show the water tank condition, 16x2 LCD is used.

There are twelve switches on MATLAB GUI. These switches are used to control lighting systems (interior light, exterior light, running light and street light), cooling systems (aircon1, aircon2, fan1 and fan2), home appliances, garden sprinkler and water pump.

2. HARDWARE IMPLEMENTATION

The required hardware components are listed as follows:

- Arduino UNO
- DHT11 Sensor
- PIR Sensor
- Ultrasonic Sensor
- 16x2 LCD
- Buzzer

2.1 Arduino UNO

The Arduino UNO is an open-source microcontroller board based on the Microchip ATmega328P microcontroller. [7] Arduino UNO reads inputs from all sensors and writes output to MATLAB GUI via serial communication port.



Fig 2 Arduino UNO [7]

2.2 DHT11 Temperature and Humidity Sensor

To measure the surrounding air, DHT11 uses a capacitive humidity sensor and a thermistor. [8] The output pin of DHT11 sensor is connected to A0 pin of Arduino UNO.

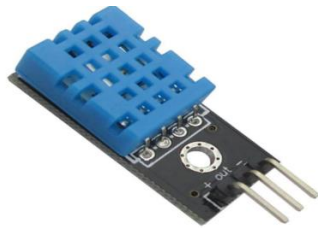


Fig 3 DHT11 Temperature and Humidity Sensor [8]

2.3 Passive Infrared (PIR) Sensor

Infrared (IR) light radiating from objects in its field of view is measured by PIR sensor. [1] The output pin of PIR sensor is connected to A1 pin of Arduino UNO.



Fig 4 PIR Sensor [1]

2.4 Ultrasonic Sensor

An ultrasonic transmitter transmits the ultrasonic wave. When this wave touches any material, it gets reflected back toward the sensor. The reflected wave is received by the ultrasonic receiver module. [4] The ultrasonic sensor works with the following formula:

$$\text{Distance} = \text{Speed} \times \text{Time} \quad (1)$$

The trigger pin of ultrasonic sensor is connected to pin 2 of Arduino UNO whereas echo pin is connected to pin 3.



Fig 5 Ultrasonic Sensor [4]

2.5 Buzzer

A buzzer or beeper is an audio signaling device. [5] Buzzer is connected to pin 4 of Arduino UNO to act as an alarm.



Fig 6 Buzzer [5]

3. SOFTWARE IMPLEMENTATION

Software requirements for the proposed system are as follows:

- Arduino Integrated Development Environment (IDE)
- MATLAB IDE
- ArduinoIO.zip

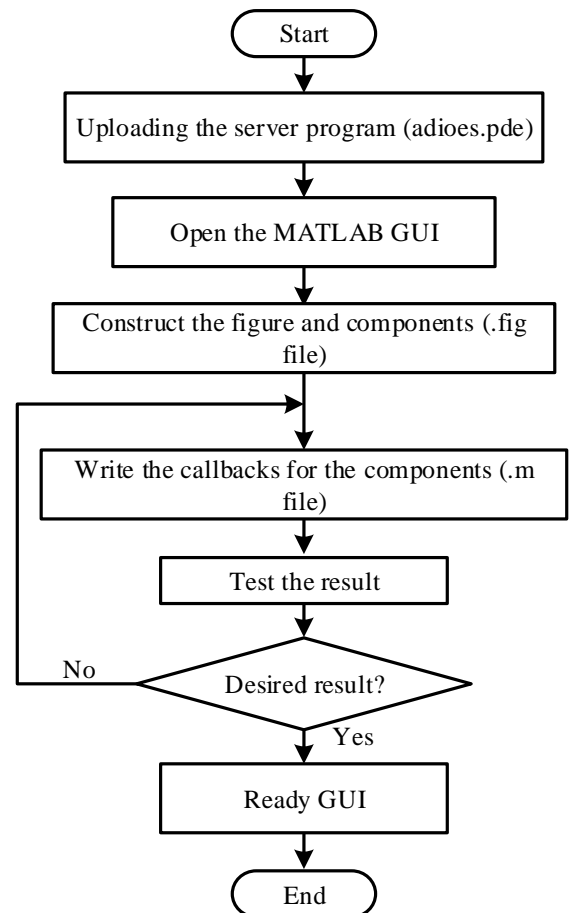


Fig 7 Flowchart of MATLAB GUI Creation

Fig 7 shows the flowchart of MATLAB GUI creation. First of all, the server program (adioes.pde) is uploaded into Arduino UNO. After that, it is needed to open MATLAB GUI. Then the figure and components are constructed as a file (.fig). Next the callbacks for components are written as a file (.m). And then the script is run to test the result. If the desired result is not achieved, the (.m) script file will be rewritten. After achieving the desired result, the GUI is ready to use.

Home control and monitoring system is initialized in the command window as shown in Fig 8 and the system initialization in the GUI is shown in Fig 9.

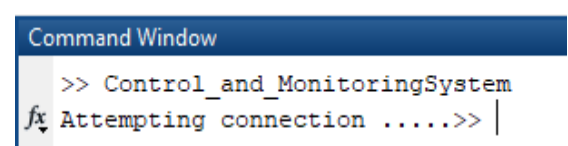


Fig 8 System Initialization (in command window)

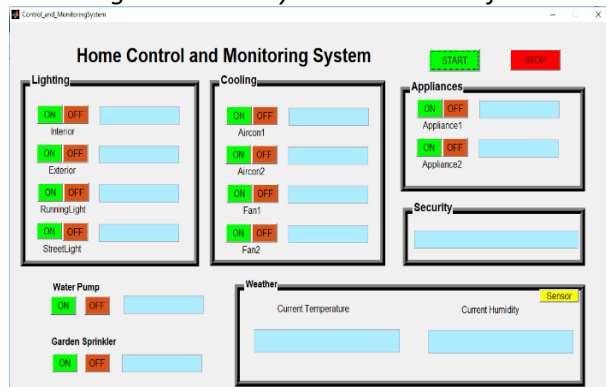


Fig 9 System Initialization (in GUI)

Fig 10 shows the complete connection between Arduino and MATLAB.

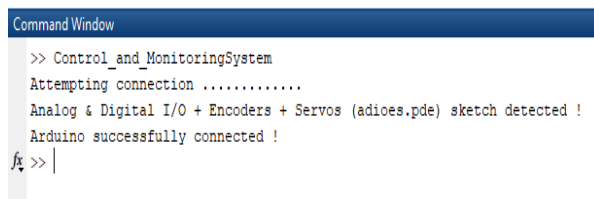


Fig 10 Interfacing Arduino with MATLAB

4. EXPERIMENTAL RESULTS

MATLAB GUI is the main heart of home control and monitoring system. There are seven panels in MATLAB GUI. They are lighting panel, cooling panel, water pump panel, garden sprinkler panel, security panel and weather panel. First of all, "START" button is pressed to use the GUI control.

There are twelve switches on the GUI. Lighting panel consists of four switches for light control. In cooling panel, there are four switches to switch on or off cooling devices. Appliances panel consists of two switches for home appliances such as TV, refrigerator, etc. The remaining two switches are used for water pump and garden sprinkler. On/Off condition of the switches will be displayed in the text boxes beside the switches.

Security panel will display movement detection condition which is received from PIR sensor. Temperature and humidity levels in home will show on weather panel in MATLAB GUI. To exit the GUI control, "STOP" button is pressed.

Fig 11 shows the system welcome message on the LCD after connecting an Arduino with MATLAB GUI.



Fig 11 Welcome Message

4.1. Temperature and Humidity

To achieve current temperature and humidity reading, sensor button on weather panel is pressed after initializing GUI. The result of this condition is shown in Fig 12.

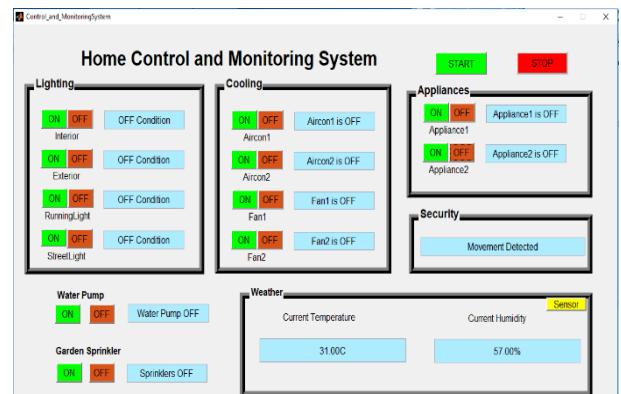


Fig 12 Real Time Temperature and Humidity Result

4.2 Water Level Detection

If the 'ON' button on the water pump panel is pressed, the water pump is turning on to fill the water. At the same time, LCD will display "Pump is ON" message and 'ON' state blue LED will turn on as shown in Fig 13.

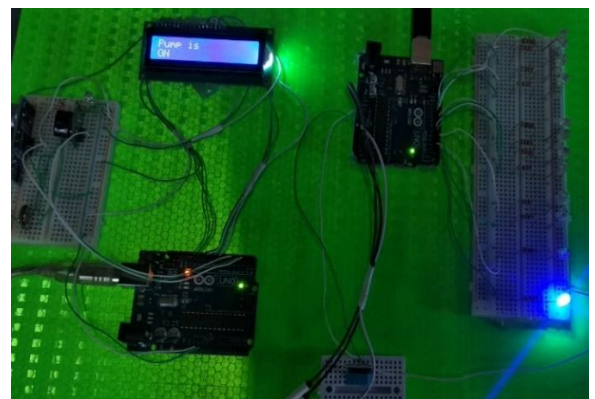


Fig 13 Water Pump Condition (ON state)

Red LED will be turned on when the water tank is full of water. The alarm message of this condition is shown in Fig 14.



Fig 14 Alarm Message to Switch off the Water Pump

From the specifications of PIR sensor, the sensitivity range is up to six meters in detection range ($110^\circ \times 70^\circ$). From the experimental results, accurate detection is received within five meters in detection range ($110^\circ \times 70^\circ$).

The movement detection message which is received from the PIR sensor via Arduino is displayed on MATLAB GUI.



Fig 15 PIR Sensor Condition: (a) No Movement
 (b) Movement Detected

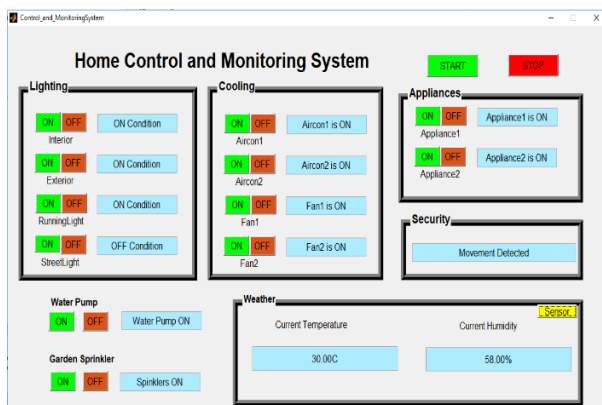


Fig 16 Movement Detected Condition (in GUI)

When all control units (lighting, cooling, and appliances) are pressed 'ON', ten LEDs will be turned on as in Fig 17.

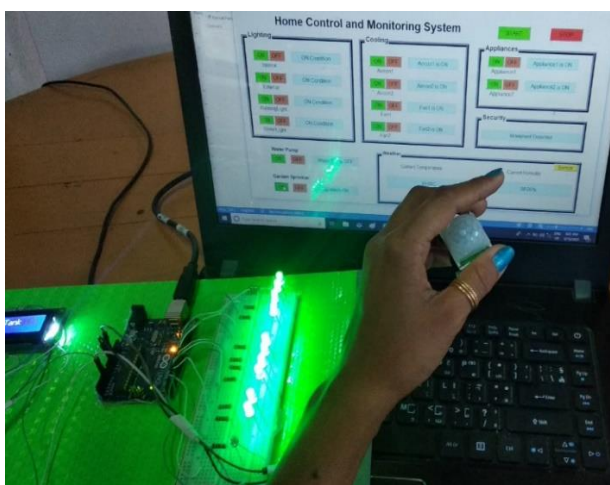


Fig 17 Movement Detected Condition



Fig 18 Overall Home Control and Monitoring System

5. CONCLUSIONS

The proposed home control and monitoring system using MATLAB GUI was designed and constructed. After constructing the overall system, the effective output was achieved from the experimental results. It is suitable for busy people and found working satisfactorily. For this reason, it is a useful system for citizens who work their relevant office's duties from home during the COVID-19 crisis. This system can be further extended to provide automatic controlled feature. For home security, it can be extended to include such as fire alarm, smoke detection, etc.

ACKNOWLEDGEMENT

The author wishes to express her deep gratitude to Dr. Zin Ma Ma Myo, Professor and Head, Department of Electronic Engineering, Technological University (Banmaw), for her encouragement and invaluable advice throughout in writing this paper. A special note of thanks is also intended all who helped her with necessary assistance for this paper.

REFERENCES

- [1] Adafruit Industries, "Adafruit Learning System, PIR Motion Sensor", 2011.
- [2] A. Elshafee and K. A. Hamed, "Design and Implementation of a WiFi Based Home Automation System," World Academy of Science, Engineering and Technology, pp. 2177-2180, 2012.
- [3] A. Z. Alkar and U. Buhur, "An Internet based wireless home automation system for multifunctional devices," Consumer Electronics, IEEE Transactions on, vol. 51, pp. 1169-1174, 2005.
- [4] Components 101, 18th September, ultrasonic-sensor-working-pinout-datasheet Available: <https://components101.com/ultrasonic-sensor-working-pinout-datasheet>, 2017.
- [5] Components 101, 27th September, buzzer-working-pinout-datasheet Available: <https://components101.com/buzzer-working-pinout-datasheet>, 2017.

- [6] Deepali Javale, Mohd. Mohsin, Shreerang Nandanwar, and M. Shingate, "Home Automation and Security System Using Android ADK," *International Journal of Electronics Communication and Computer Technology*, vol. 3, pp. 382-385, 2013.
- [7] Massimo Banzì, "Getting Started with Arduino", second edition, 2011.
- [8] Pixel Electric Engineering Company Limited, dht11-temperature-humidity-sensor. Available: <https://pixelelectric.com/dht11-temperature-humidity-sensor>, 2020.
- [9] Rajesh Singh, Anita Gehlot, Bhupendra Singh, Sushabhan Choudhury, "Arduino meets MATLAB: Interfacing, Programs and Simulink, Bentham Science Publishers, 2018.
- [10] R. Piyare and M. Tazil, "Bluetooth based Home Automation System using Cell Phone," in *Consumer Electronics (ISCE)*, 2011 IEEE 15th International Symposium on, pp. 192-195, 2011.

AUTOMATIC MYANMAR PAPER CURRENCY RECOGNITION USING ALEXNET MODEL

Lei Lei Win⁽¹⁾, Khin Myo Aye⁽²⁾

⁽¹⁾Technological University (Hmawbi), Myanmar

⁽²⁾ Technological University (Hmawbi), Myanmar

Email: lailaiwin506@gmail.com

ABSTRACT: This paper presents the recognition of different Myanmar Paper Currencies using deep learning CNN (AlexNet) model. Paper currency recognition depends on the currency note characteristics of a particular country. These currencies are different with their features such as the size of the banknotes, color, shape, texture, height, width, etc. For this system, the most common Myanmar banknotes such as 100, 200, 500, 1000, 1000new, 5000, 10000 kyats are used. A Banknotes dataset including these currencies is created by our own, where the images were taken by using smartphone camera. In this system, classification algorithm AlexNet model is used for recognizing different classes of Myanmar paper currencies. AlexNet model based on deep convolutional neural network was trained our image data in a Deep Learning framework – Google Colab. This system is implemented by using Python programming language. Experimental results show a high accuracy of 99.2% in a confusion matrix on the different types of Myanmar paper currencies recognition. This system can be used without human intervention and replacing humans for some kinds of business such as goods selling, public transport, banks, etc.

KEYWORDS: *Deep Learning, Artificial Intelligence, Google Colab, AlexNet, Currency Recognition.*

1. INTRODUCTION

Currently, paper currency recognition system has evolved as one of the most common applications of pattern recognition. Pattern recognition is important field in artificial intelligence and computer vision [1]. The previous methods used by other researchers are as follows. “Myanmar Paper Currency Recognition Using GLCM and k-NN” uses Gray Level Co-occurrence Matrix (GLCM) method as textural feature extraction and k-Nearest Neighbors (k-NN) as recognition method. This paper consists of 5 classes of currency notes which are 100, 200, 500, 1000, 5000 kyat notes to read their face values. The recognition accuracy of this system is 99.2% [1]. “Correlation-based Recognition System for Myanmar Currency Denomination” presents the computing of correlation coefficient to compare the similarity for each currency value template via image processing steps in Matlab environment. This paper uses two kinds (fresh and medium) of each 7 types of denomination. In this paper, the system is sensitive for

any orientations of input currency images [2]. “Feature Extraction for Myanmar Paper Currency Denomination Using CIELUV” uses the CIELUV color space for feature extraction and finally shows the output result. This method is extracted the feature for the front side and back side of Myanmar paper currencies (kyats) a different classes. This system is implemented by using MATLAB programming language and include user friendly interface [3].

After learning above papers, machine learning classification algorithms are used for classification currency images. So, feature extraction is manually crafted by human. When the user has not been properly cropped the currency image area, the performance of the currency recognition system will be decreased. In the proposed work, there is no need human crafted feature extraction technique because the classification algorithm used in this system is Deep learning CNN. This system eliminates the manual feature extraction and learns directly along with the classification tasks. It can also satisfy the orientation of input image. In this paper, one of the most effective models of CNN called AlexNet model is used for detecting and classifying seven different classes of Myanmar Paper Currencies. The overall block diagram of the system is as shown in Fig. 1.

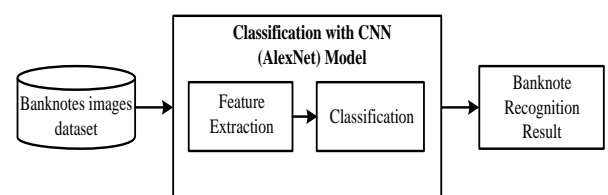


Fig 1. Overall block diagram of the system

2. THEORETICAL BACKGROUND

2.1 Deep Learning

Deep learning is a subset of artificial intelligence (Fig.2) that acts like human brain for handling data and generating patterns which helps in decision making. The structure of deep learning comes from artificial neural networks [4]. The term “deep” refers to the number of layers in the network—the more layers, the deeper the network. Most deep learning methods used neural network architectures [8].

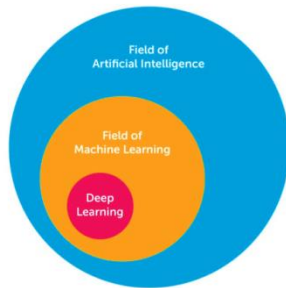


Fig 2. The relation between artificial intelligence, machine learning and deep learning [9]

Deep learning techniques overcome the problem of feature selection by not requiring pre-selected features but extracting the significant features from raw input automatically for a problem in hand as shown in (Fig.3). It consists of a collection of processing layers that can learn various features of data through multiple levels of abstraction [5]. Deep learning has become very popular recently because it is highly accurate. Convolutional Neural Network (ConvNet or CNN) is a category of deep neural networks which has proven to be very effective in areas such as image recognition and classification [6].

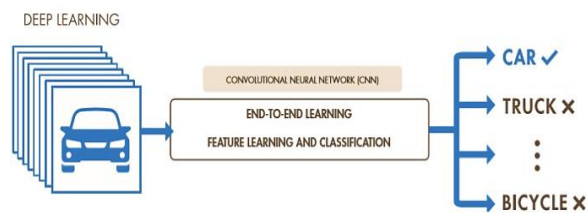


Fig 3. Deep Learning [8]

2.2 Convolutional Neural Networks (CNN)

Convolutional neural networks (CNN) are a specific type of neural network systems that are particularly suited for computer vision problems such as image recognition. In such tasks, the dataset is represented as a 2-D grid of pixels (Fig.4). [7]

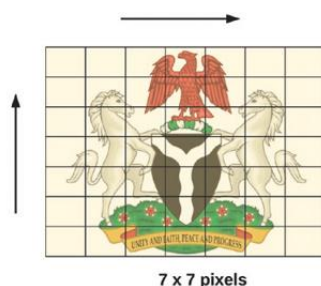


Fig 4. 2-D representation of an image [7]

An image is depicted in the computer as a matrix of pixel intensity values ranging from 0 to 255. A colored image consists of three channels, red, green, and blue, with each channel also containing pixel intensity values from 0 to 255. A colored image has a matrix shape of [height x width x channel]. In Fig.5, we have an image of shape [10 x 10 x 3] indicating a 10 x 10 matrix with three channels. [7]

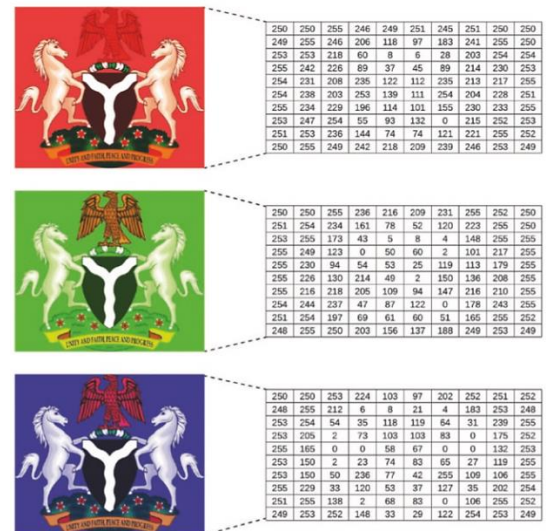


Fig 5. Colored image with matrix representation [7]

Convolutional neural networks are composed of three fundamental types of layers:

- Convolutional layer
- Pooling layer
- Fully connected layer

2.3 AlexNet Model

AlexNet [Krizhevsky et al., 2012] was the first large-scale CNN model which led to the resurgence of deep neural networks in computer vision. This architecture won the ImageNet Large- Scale Visual Recognition Challenge (ILSVRC) in 2012 by a large margin. It consists of a total of eight parameter layers among which the five initial layers are convolutional layers, while the later three layers are fully connected layers. The final fully connected layer (i.e., the output layer) classifies an input image into one of the thousand classes of the ImageNet dataset, and therefore contains 1,000 units. Note that dropout is applied after the first two fully connected layers in the AlexNet architecture, which leads to a reduced over-fitting and a better generalization to unseen examples. Another distinguishing aspect of AlexNet is the usage of ReLU nonlinearity after every convolutional and fully connected layer, which substantially improves the training efficiency compared to the traditionally used tanh function. This architecture has about 60M parameters [6]. The AlexNet architecture is as shown in Fig. 6.

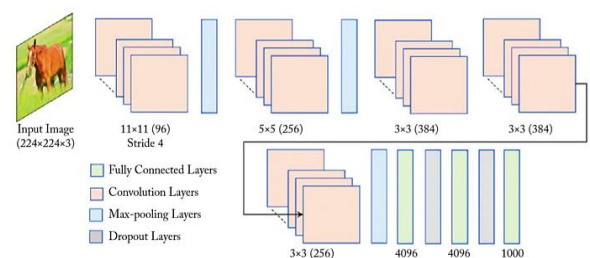


Fig 6. AlexNet architecture [6]

Google Colaboratory or “Colab” for short, is a free cloud service hosted by Google to encourage Machine Learning and Artificial Intelligence research, where often the barrier to learning and success is the requirement of tremendous computational power. Colab allows anybody to write and execute arbitrary python code through the browser, and is especially well suited to machine learning, data analysis and education. More technically, Colab is a hosted Jupyter notebook service that requires no setup to use, while providing free access to computing resources including GPUs. [10]

3. Proposed Method

This system is mainly implemented by three steps, dataset creation, training with AlexNet model, testing and classification. This system is implemented by using python programming language on Google Colab framework. The system needs many photos of Myanmar banknotes because it is an AI system. This system uses 7 different types of Myanmar banknotes such as 100, 200, 500, 1000, 1000new, 5000, and 10000 kyats. The methodology of implementation steps for this system is as shown in Fig.7.

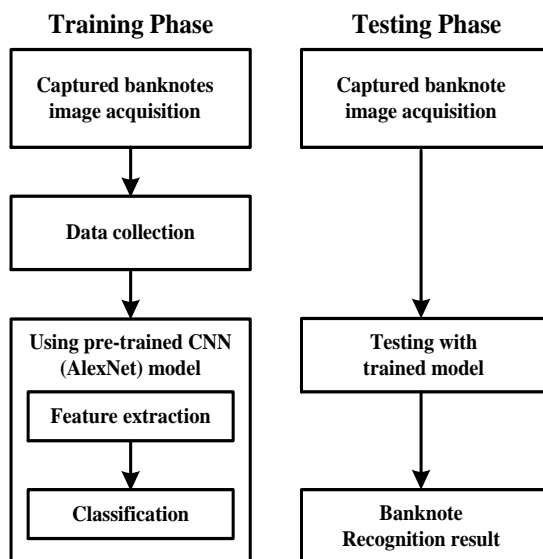


Fig 7. Methodology of implementation

3.1 Dataset

In this system, different Myanmar paper currency images are firstly captured with different rotations and angles by using smartphone's camera. These images are added to the Banknotes dataset as shown in Fig.8. Banknotes dataset consists of 420 images grouped into 7 categories. The 7 categories are: 100, 200, 500, 1000, 1000new, 5000 and 10000 kyats. Each class has 60 images. Those images are uploaded in the Google Drive. The 70% of images (294 images) from Banknotes dataset are added to the training dataset. The 30% of images (126 images) are used for validation or prediction.

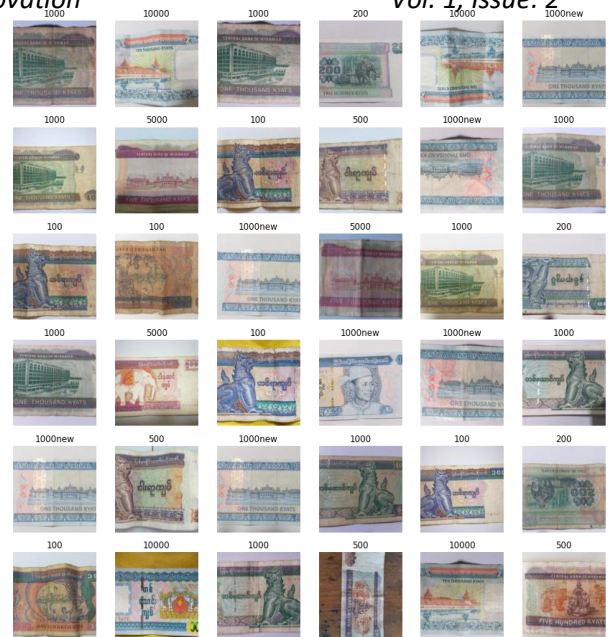


Fig 8. Example images of Banknotes dataset

3.2 Training the Network

In the training phase, the images in the Banknotes dataset are directly fed to AlexNet model pre-trained on Google Colab framework. AlexNet model is one of the most popular image processing architectures of Deep Learning Neural Network. The training process is done for 7 classes of different banknotes to recognize accurately. The banknotes images are randomly selected from the Banknotes dataset to be trained in AlexNet model. Then the model is trained for 5 epochs by using one-fit-cycle. After training 5 epochs, the results are as shown in Table.1.

Table 1. Pre-training AlexNet model for 5 epochs

epoch	train_loss	valid_loss	error_rate	time
0	2.724516	2.656038	0.809524	00:06
1	1.781264	0.736733	0.261905	00:06
2	1.183444	0.181453	0.039683	00:06
3	0.864083	0.050015	0.023810	00:06
4	0.668821	0.023573	0.007937	00:06

According to the above result, error_rate at epoch 0 is higher than error_rate at epoch 4. So, higher the number of epochs lower the error_rate of recognition.

4. RESULTS AND DISCUSSION

The overall Myanmar Paper Currency Recognition problem is divided into three sections. Firstly, a dataset is created by own captured banknote images. Secondly, the CNN network is trained to classify different banknotes by using deep learning classifier called AlexNet model. Finally, test images are randomly given to the network to evaluate the accuracy of the system with a confusion matrix. It is observed that the

system correctly recognizes different Myanmar Paper Currencies with accuracy of 99.2% on Banknotes dataset. Fig.9 shows the confusion matrix of recognition results.

$$\text{accuracy} = \frac{\text{number of correct prediction}}{\text{number of total prediction}} \times 100 \quad (1)$$

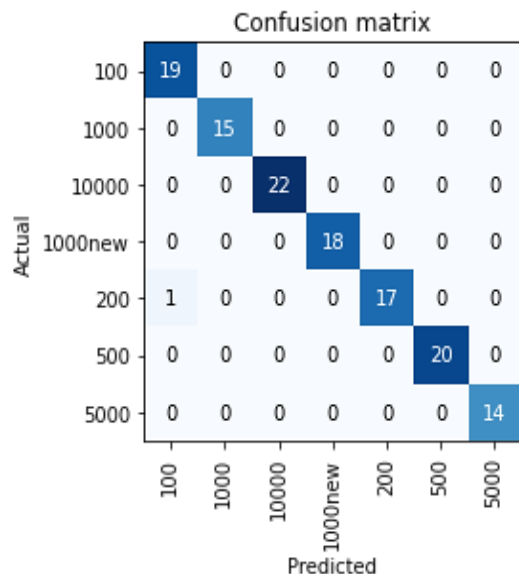


Fig 9. Confusion matrix

The confusion matrix shows the actual value and predicted value of each banknote class. Actual images are randomly taken from the validation dataset to compare with the training dataset. For example, actual 19 images of 100 kyats are predicted correctly. After actual 18 images of 200 kyats are predicted, 17 images are predicted correctly but 1 image is predicted incorrectly. According to the confusion matrix, the accuracy of the system is obtained by training different Myanmar Currencies from the training datasets on the AlexNet model. After training process, the resulting classification output is as shown in Table.2.

Table 2. Myanmar paper currency classification output

Kyats	100	200	500	1000	1000new	5000	10000
Quantity	19	18	20	15	18	14	22
True	19	17	20	15	18	14	22
False	00	01	00	00	00	00	00
Accuracy (%)	100	94.4	100	100	100	100	100
Total accuracy (%)	99.2						

5. CONCLUSIONS

In this paper, a pre-trained AlexNet model based on CNN architecture is utilized for different Myanmar Paper Currencies recognition with high accuracy. The experimental results showed the overall accuracy of 99.2% on currencies recognition. CNN's AlexNet model eliminates the manual feature extraction and learns directly along with the classification tasks. From this experiment, orientation does give effect to the performance of pre-trained model (AlexNet) of Convolutional Neural Network (CNN). The system can extract features for the front side and back side of different Myanmar Currencies images. The accuracy of this recognition system depends on number of training time and other CNN models. Thus, other researches will be needed.

ACKNOWLEDGEMENT

The author would like to acknowledge Dr. Kay Thi Lwin, Rector of Technological University (Hmawbi), for her kind permission to do this research work. And the author also would like to acknowledge Dr. Wai Phyo Aung, Head of the department and all the teachers from Department of Electronic Engineering. The author especially would like to express her thanks to supervisor, Daw Khin Myo Aye, Associate Professor, Department of Electronic Engineering, for her motivation and encouragement to complete this paper in time.

REFERENCES

- [1] Khin Nyein Nyein Hlaing, Anilkumaar Kothalil Gopalakrishnan, "Myanmar Paper Currency Recognition Using GLCM and k-NN", In: Second Asian Conference on Defence Technology (ACDT), Bangkok, Thailand, 2016 IEEE.
- [2] Thi Thi Soe*, Zarni Sann**, "Correlation-based Recognition System for Myanmar Currency Denomination", In: International Journal of Scientific and Research Publications (IJSRP), Volume 8, Issue 8, August 2018.
- [3] War War Tun, Nay Win Zaw, Kyu Kyu Thin, "Feature Extraction for Myanmar Paper Currency Denomination Using CIELUV", International Conference on Science and Technology for Sustainable Development (ICSTSD), Nov 4-5, Pg-195@ 2019.
- [4] Emine Cengil and Ahmet Cinar, "Classification of Human Driving Behavior Images using Convolutional Neural Network Architecture", In: Springer Nature Switzerland AG 2019, H. Perez Garcia et al. (Eds.): HAIS 2019, LNAI 11734, pp.264-274, 2019.

- [5] Sakshi Indoliaa,*, Anli Kumar Goswami.b, S.P.Mishrab, Pooja Asopaa, "Conceptual Understanding of Convolutional Neural Network- A Deep Learning Approach", International Conference on Computational Intelligence and Data Science (ICCIDS 2018), Procedia Computer Science 132 (2018) 679-688.
- [6] Salman Khan, Hossein Rahmani, Syed Afaq Ali Shah, Mohammed Bennamoun, "A Guide to Convolutional Neural Networks for Computer Vision", 2018.
- [7] Ekaba Bisong, "Building Machine Learning and Deep Learning Models on Google Cloud Platform: A Comprehensive Guide for Beginners", ISBN-13 (electronic): 978-1-4842-4470-8, 2019.
- [8] <https://www.mathworks.com/discovery/deep-learning.html>
- [9] <https://mc.ai/data-scientist-vs-machine-learning-vs-artificial-intelligence-vs-deep-learning/amp/>
- [10] <https://research.google.com/colaboratory/faq.html>

HOME APPLIANCES CONTROL SYSTEM WITH ESP8266 MICROCONTROLLER

Win Yu Cho ⁽¹⁾, Ni Ni San Hlaing⁽²⁾

⁽¹⁾Technological University (Kyaukse), Myanmar

⁽²⁾Technological University (Kyaukse), Myanmar

Email: winyuchogyic@gmail.com, maninisanhlaing@gmail.com

ABSTRACT: This paper presents the design and implementation of home appliances control using IoT. Nowadays, the smart home technology has become popular in the environment and around the world. In the modern age, the home appliances control using IoT is the most updated technology. This system is intended to control home appliances ON and OFF states over mobile phones or PC (Personal Computer) through internet when the user reached away from the home. This home appliances control system is especially implemented by using ESP8266 NodeMCU microcontroller in order to perform wireless control over it. Moreover, MIT App software is also used as command device for giving the inputs to the microcontroller. This is designed and implemented to control the home appliances such as three lights ON/OFF states, Fan ON/OFF states and Rice Cooker ON/OFF states. Anyone can control the home appliances from the remote area by applying this system.

KEYWORDS: ESP8266 Microcontroller, IoT, MIT Application, Mobile Phone, Home Appliances

1. INTRODUCTION

Home automation is the process of controlling home appliances automatically using various control techniques. Home automation may include control of light, fans, appliances, and other systems, to provide more convenience, comfort, power cutting down and security.

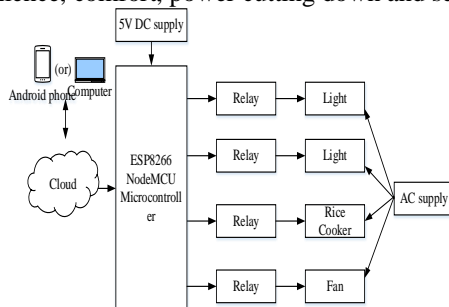


Fig 1. The Block Diagram of IoT Based Home Appliances Control System

There are various techniques to control home appliance such as IOTs based home automation over the cloud, home automation under Wi-Fi through android apps from any smartphone, Arduino microcontroller-based automation, home automation by android application based remote control, home automation using digital control, RF based home automation system and touch screen based home automation [1-7]. Among these technologies, the IoT based home appliances control is implemented for this paper.

The block diagram of this system is shown in Fig 1. From android mobile phone or personal computer (PC), user sends commands data to NodeMCU (also called ESP8266 microcontroller) through internet and the 5V power is supplied to operate the microcontroller and relay modules. By using these commands, ESP8266 NodeMCU microcontroller sends signal to relay modules in home. These relay modules operate as switches to turn ON and turn OFF the Light1, Light2, Fan and Rice Cooker.

2. DESIGN AND IMPLEMENTATION OF THE SYSTEM

This system is designed and implemented with ESP8266 NodeMCU microcontroller to control the home appliances system and it is the heart of this system. ThingSpeak server is used as a cloud service interface between the user and the home for this system. And then, MIT App software is also used as command device for giving the inputs to the microcontroller. It is installed on the mobile phone and create the control module in this application. The driver circuits are also used to drive home appliances.

2.1 Power Supply Circuit

The most one important of this system is 5V power supply and it can support that the microcontroller can work normally by taking power from the power supply circuit. Since the microcontroller needs the regulated 5 volts power supply, it is implemented first. A power supply is built by using a transformer, rectifier and regulator. The step-down transformer is used to set down the AC voltage to desired amplitude, then rectifying that AC voltage, filtering with a capacitor and the desired DC voltage is generated by using IC regulator. The LM323 regulator IC is used to generate 5V DC.

The circuit diagram of 5V power supply circuit is shown in Fig 2.

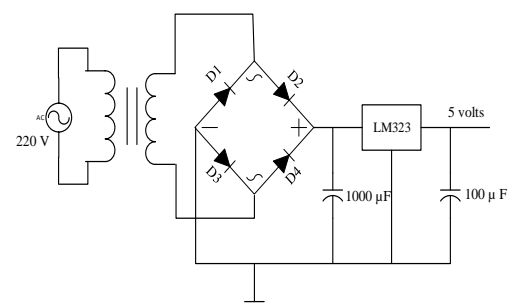


Fig 2. The 5V Power Supply Circuit

The hardware implementation of 5V power supply is described in Fig 3.

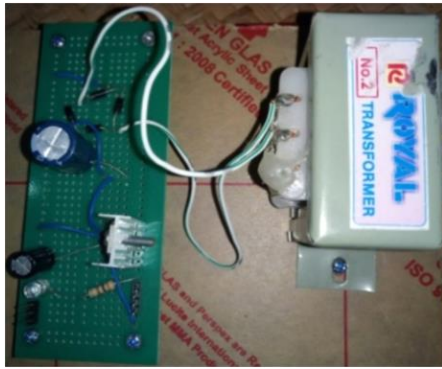


Fig 3. The Implementation of 5V Power Supply Circuit

2.2 Implementation of the Overall System

This home appliances control system is implemented with ESP8266 NodeMCU. ThingSpeak Channel is used as cloud server in the system and is also used to display the information of home appliances “ON” state and “OFF” state. The MIT App Inventor software application is used as control device (i.e. switch) for Home Appliance Control System. Driver circuits for AC loads are connected to D1, D2, D3, D4, D5, D6 and D7 which are pin3, pin4, pin 5, pin6, pin13, pin12 and pin11 of ESP8266 NodeMCU microcontroller. So, D1, D2, D3, D4, D5, D6 and D7 are set as output pins in the software. Four 5V relays are connected to AC socket where loads can connect. The Overall Circuit Diagram for Home Appliances Control System is shown in Fig 4.

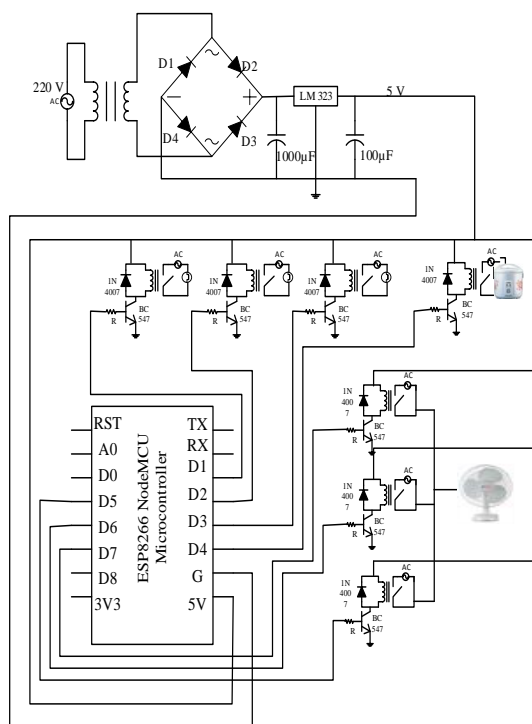


Fig 4. The Overall Circuit Diagram for Home Appliances Control System

3. CONTROL BUTTONS IMPLEMENTATION ON MIT APPLICATION

Firstly, to create the block, label text is taken from the user interface to write the project name (e.g. Home Appliance Control Using IOT). And then, to make the button click, button text is taken from the user interface to the desired home screen. If the name of the button is

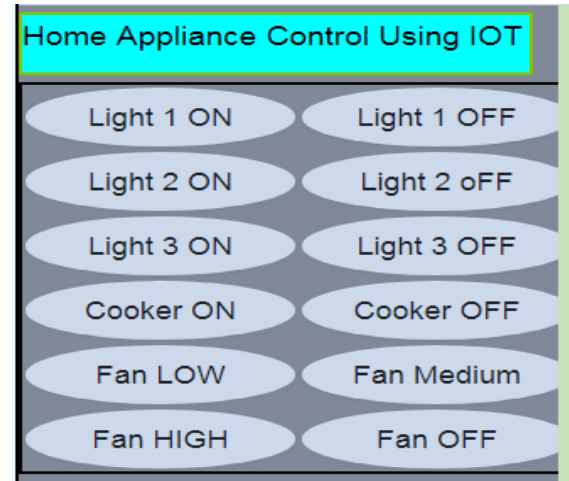


Fig 5. Implementation Control Buttons on MIT Application in Android Phone

changed, this button is clicked and the desired name is assigned in the text from the properties box. The font size, the button shape and the colour are changed in the properties box. In this system, the font size is 20, the button shape is oval shape and the colour is default. The implementation of MIT application for Home Appliance Control System is shown in Fig 5.

4. SYSTEM FLOW CHART

In the microcontroller side, when the system is powered, ESP 8266 NodeMCU microcontroller will try to connect to Wi-Fi hotspot of predefined ssid and password. Then it will turn off all relays. After initiating, it will read the last value of field 1, field 2, field 3, field 4 and field 5 from ThingSpeak channel of predefined ThingSpeak number. If the value of field is 1, it will turn on the associated relay which is connected with the home appliance. If the value of field is 0, it will turn off the associated relay which is relay “OFF” state. The flow chart of the whole system is shown in Fig 6.

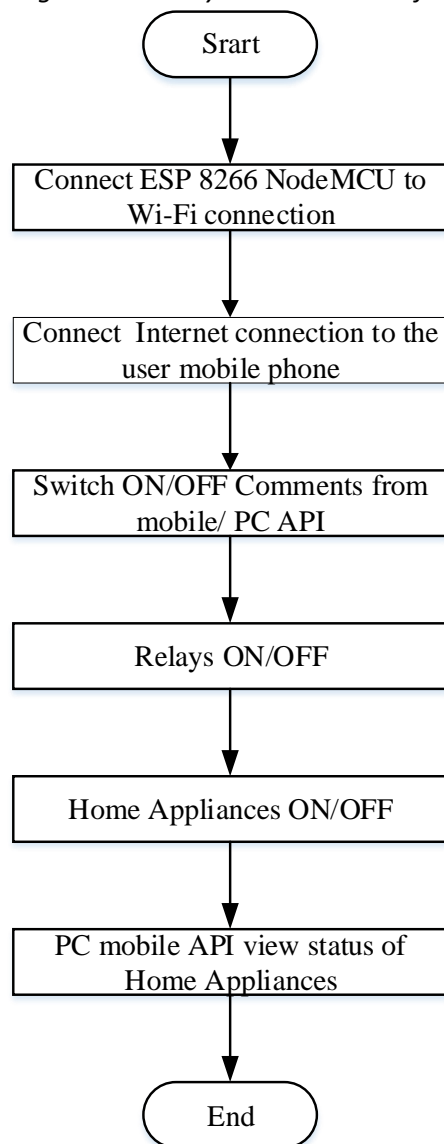


Fig 6. The Flow Chart of the Overall System

According to the flow chart of this system, firstly the user must connect the ESP 8266 NodeMCU with WiFi and the mobile phone or PC must have internet connection. And then, the user can give commands to control the home appliances such as Light1, Light2, Light3, Fan and Rice Cooker via mobile home or PC. After giving commands to the system, the microcontroller receives and sends those commands to the relay in order to do ON/OFF conditions of the desired appliances. At this time, the desired home appliances are running according to the user's commands. Finally, the user can view the running conditions of the home appliances from the mobile phone or PC.

5. TEST AND RESULTS

This home appliances control system is applied 5V DC power supplied to the microcontroller and relays. All appliances which are used in this system are applied by AC power. They are three Light Bulbs, Fan and Rice Cooker. The testing and results of all appliances are shown in this section. Firstly, the testing of the 5V power supply by using a meter is illustrated in Fig 7.



Fig 7. Testing of 5V Power Supply



Fig 8. The Result of Light 1 ON

The buttons which are created in MIT application must be pressed to give the commands to the controller in order to control the home appliances ON/OFF states. If the user presses the button of "Light 1 ON", the Light 1 will be in the ON state. The result of the Light 1 ON state is shown in Fig 8. If the user presses the button of "Light 1 OFF", the Light 1 will be in the OFF state. The result of the Light 1 OFF state is shown in Fig 9.



Fig 9. The Result of Light 1 OFF

Similarly, the other Light 2 and Light 3 can also be tested in this way. They can perform very well according to given control commands. The result of Light 2 and Light 3 ON/OFF states are shown in Fig 10, Fig 11, Fig 12 and Fig 13.



Fig 10. The Result of Light 2 ON State



Fig 11. The Result of Light 2 OFF State



Fig 12. The Result of Light 3 ON



Fig 13. The Result of Light 3 OFF

If the user presses the button of “Cookeer ON”, the rice cooker will be in the ON state. The result of the rice cooker ON state is shown in Fig 14.



Fig 14. The Result of Rice Cooker ON

In the same way, if the user presses the button of “Cookeer OFF”, the rice cooker will be in the OFF state. The result of the rice cooker OFF state is shown in Fig 15.



Fig 15. The Result of Rice Cooker OFF

The AC Fan will be ON state with low speed if the user presses the button of “Fan Low”. The AC Fan will be ON state with median speed if the user presses the button of “Fan Median”. The AC Fan will be ON state with low speed if the user presses the button of “Fan High”. The result of Fan ON state is shown in Fig 16.



Fig 16. The Result of Fan ON

If the user presses the button of “Fan OFF”, the Fan will be in OFF state. The result of Fan OFF state is shown in Fig 17.



Fig 17. The Result of Fan OFF

This system can also be controlled from the remote area. However, the internet connection is necessary for both the user and home appliances control circuit. The working conditions of this home appliances control system can be seen on PC via Thing speak sever. It has little delay to see the working condition graph because so many users use that sever.

6. CONCLUSIONS

In this system, three different types of home appliances are used to test the implemented circuit. They are three bulbs, fan and rice cooker and they all are AC loads. The bulbs are named as Light 1, Light 2 and Light 3 in this system. The rice cooker is named as Cooker. In addition, the fan is also tested with different speeds. Therefore, it is also named as Fan Low, Fan Median and Fan High. The operations of these appliances are controlled by ON/OFF button from MIT application. These control comments are received from ESP8266 Microcontroller and fed them to the AC loads. The loads operate according to the information from the microcontroller. For this reason, the ESP8266 microcontroller is the heart of this system. However, the working condition of this system cannot be seen on the computer without any internet connection. This system can be applied in the most area around the world because it can save time and human work force.

ACKNOWLEDGMENT

The author desires to express her special thanks to Prof. Dr. Khin Htike Htike Lwin, Rector, Technological University (Kyaukse), for her encouragement and kind permission to submit this system. The author particularly wishes to acknowledge all the teachers from the Department of Electronic Engineering, Technological University (Kyaukse), for their encouragement and invaluable suggestions in the preparation of this paper.

REFERENCES

- [1] Muhammad Tanveer Riaz: “Wireless AndroidBasedHome Automation System”, Vol.2, No.1, ISSN: 2415-6698, January 2017, India.

- [2] Grezello Fernandes: “A Study on the SmartHomesUsing IOT”, pp.533-536, e-ISSN: 2278-612X, 2016.
- [3] Salahuddin Dalvi: “Home Automation Using Arduino Wi-Fi Module ESP8266”, 2016, Panvel.
- [4] Anonymous: “Studies Explore Future Demand forSmart Home System”, <http://hnn.bz/fullview?articleIndex=022101610529>, October 2016.
- [5] Ahonen: “Internet of Things- Wireless Technologiesin Home Automation Solutions”, University of Jyvaskylo, 2015.
- [6] Aeindra Myint Lwin: “Design and ImplementationofSmart Living Room Wireless Control for Safety Purpose”, Vol.4, Issue 07, ISSN 2277-8616, July 2015.
- [7] Anonymous: “Top Tips for Creating a StreamlinedSmart Home” <http://techspective.net>, August 2014.

PERFORMANCE ANALYSIS OF BILATERAL FILTER FOR MYANMAR SIGN-LANGUAGE RECOGNITION SYSTEM USING K-NN CLASSIFIER

Soe Soe Khaing⁽¹⁾, Myint Myint Yi⁽²⁾

⁽¹⁾Technological University (Hmawbi), Myanmar

⁽²⁾ Technological University (Hmawbi), Myanmar

Email: soekhaing79@gmail.com

ABSTRACT: The sign language is gesture language used by the people with the speech and hearing disabilities for communication in their daily conversation activities. Myanmar Sign- Language is the language of choice for most mute people in Myanmar. In this paper, Myanmar Sign-Language (MSL) recognition system using k-NN classifier with two types of filters is presented. The captured image frame from WebCam is smooth by bilateral filter and is converting resizing and cropping in OpenCV library and it is converted grayscale image. The noise of grayscale image is reduced by Gaussian filter. The trained data set is constructed by extracting the corresponding features of Imageset. Once the hand gestures are recognized, the text is displayed on Result Test Box and the speech is appeared on built-in speaker. This system can accomplished the translation of 31 static signs (hand gestures) into text (Myanmar alphabets) and speech to assist the mute people for teaching. This paper has mainly emphasized two case of noise reducing. Firstly, only Gaussian filter is used to reduce noise and the second is both bilateral and Gaussian filters are used. By analyzing the experimental results, percentage accuracy of the system using both bilateral and Gaussian filters is better than that using only Gaussian filter. The better accuracy MSL system can support teaching in a school for the deaf.

KEYWORDS: background subtraction, Gaussian filter, bilateral filter, k-NN classifier, Open CV, Python

1. INTRODUCTION

People with special needs or disabilities are also part of society, where they have the same right to interact and socialize with the surrounding environment. Persons with disabilities, such as deaf and speech impaired sometimes looks like a normal person. However, problems arise when communication with others, the deaf cannot hear, whereas speech impaired cannot be answered conversation. Classically, this problem can be answered, in which the deaf using hearing aids. While the speech impaired using sign language, through hand gestures or body movements. There are many different types of gestures and they are set belong to the sign languages. Each gesture already has assigned meaning and context in sign language. The sign language recognition system is approached by Sensor based and Vision based.

In Sensor Based approach, sensors were used and placed on hand and then the hand gestures data is recorded and is then further analyzed. In Vision Based approach, camera takes the image of hand gesture, extracts the main feature and recognizes it.

Image processing is the basic technique implemented in this paper. Processing involves basic image processing techniques such as detecting, denosing, gray scale image, feature extraction and recognition. A continuous real time stream of video data captured by the Webcam is the basic input to the processing system. In this paper, 31 static sign gestures using Mary Chapman School for the Deaf in Yangon that are used. System block diagram of this paper is shown in Figure 1. First, image set is constructed by collecting hand gestures from Webcam and then feature extraction from image set and dataset is constructed. In the hand gesture recognition step, the hand gesture income from Webcam and recognized the dataset. Then, the output text is shown from result text box and the built-in speaker out speech.

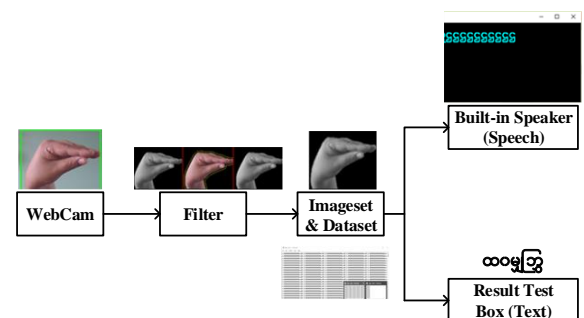


Fig 1. Overall system of this system

2. RELATED WORK

Fitrah Maharani Humaira, “Real Time SIBI Sign Language Recognition based on K-Nearest Neighbor”, LMC(leap motion controller) is able to capture the image of a hand that can automatically separates the background, then can ignore the morphological operations and hand detection can be done. Color segmentation is used to get binary images. The results of SIBI sign language recognition accuracy by using leap motion controller and k-NN performed on the 26-letter alphabet. Testing is done in real-time towards training data. In this paper is determined 3 parameter value of k nearest neighbour namely 5, 10 and 15. The test results indicate that the parameter value k =

5 has the highest accuracy (78%) compared with the $k = 10$ and $k = 15$ [1].

Muhammad Aminur Rahaman, "Real-Time Computer Vision-Based Bengali Sign Language Recognition", uses an ASUS A42F series laptop with Intel Core i3 processor and 2GB RAM. This research has used C# OpenCV wrapper as system development platform. The system uses Haar-like feature-based cascaded classifiers to detect the hand in each frame. From the detected hand area, the system extracts the hand sign based on Hue and Saturation value corresponding to human skin colour. After normalization the system converts the hand sign to binary image. Then the binary images are classified by comparing with pre-trained binary images of hand sign using k-Nearest Neighbours (k-NN) Classifier. The system is able to recognize 6 Bengali Vowels and 30 Bengali Consonants. The recognition accuracy of this system is 96.64% [2].

Priyanka Lokhande, "Data Glove for Sign Language Recognition System", consists of a glove, flex sensors, 3-axis accelerometer and ADC of microcontroller ARM LPC 2138. The hand gestures are assigned to corresponding words using flex sensors and 3-axis accelerometer. The signals are converted to digital data using comparator circuits and ADC of microcontroller ARM LPC 2138. The microcontroller matches the binary combinations with the databases and produces the speech signal. The output of the system is displayed using the speaker and LCD [3].

Reading above papers, in sensor-based approach the natural motion of hand can be damaged and complex gestures cannot be performed. In Real-Time Computer Vision-Based Bengali Sign Language Recognition, HSV is used to detect hand gesture but weak in skin colour detect. So, background subtraction is considered to apply. In Real Time SIBI Sign Language Recognition based on k-Nearest Neighbour, LMC is used to capture hand gesture but the system use Webcam and background subtraction is used to detect hand gesture. In this paper, the bilateral and Gaussian filters are used to reduce the noise for hand gesture images.

3. THEORETICAL BACKGROUND

MSL is a vision based recognition system. In this system, object detection, denoising, feature extraction and classification process are included.

3.1 Moving Object Detection (Background Subtraction)

Background subtraction is a widely used approach for detecting moving objects in videos from static cameras. The rationale in the approach is that of detecting the moving objects from the difference between the current frame and a reference frame, often called "background image", or "background model". Background subtraction is mostly done if the image in question is a part of a video stream. Background subtraction provides important cues for numerous applications in computer vision, for example surveillance tracking or human poses estimation.

Background subtraction is generally based on a static background hypothesis which is often not applicable in real environments. With indoor scenes, reflections or animated images on screens lead to background changes. Similarly, due to wind, rain or illumination changes brought by weather, static backgrounds methods have difficulties with outdoor scenes [4].

3.2 Denoising Process

Image filtering is used to remove noise. Image filters can be classified as linear or nonlinear. Linear filters are also known as convolution filters as they can be represented using a matrix multiplication [5].

2.2.1 Gaussian filter

In this paper, Gaussian filter is used to reduce the noise and smooth image. A Gaussian filter is a linear filter. It's usually used to blur the image or to reduce noise. Using two of them and subtract, you can use them for "unsharp masking" (edge detection). The Gaussian filter alone will blur edges and reduce contrast. The Median filter is a non-linear filter that is most commonly used as a simple way to reduce noise in an image. Its claim to fame (over Gaussian for noise reduction) is that it removes noise while keeping edges relatively sharp. The one advantage a Gaussian filter has over a median filter is that it's faster because multiplying and adding is probably faster than sorting [6].

3.2.2 Bilateral filter

A bilateral filter is a non-linear, edge-preserving, and noise-reducing smoothing filter for images. It replaces the intensity of each pixel with a weighted average of intensity values from nearby pixels. This weight can be based on a Gaussian distribution. Crucially, the weights depend not only on Euclidean distance of pixels, but also on the radiometric differences (e.g., range differences, such as color intensity, depth distance, etc.). This preserves sharp edges [7]. An example of smoothing process using Gaussian filter is shown in Figure 2.



(a) Original Image

(b) After Filtering Image

Fig 2. The Filtering Process using Gaussian Filter [7]

3.3 Feature Extraction

In machine learning, pattern recognition and in image processing, feature extraction starts from an initial set of measured data and builds derived values (features) intended to be informative and non-redundant, facilitating the subsequent learning and generalization steps, and in some cases leading to better human interpretations. Feature extraction is related to dimensionality reduction. When the input data to an algorithm is too large to be processed and it is suspected to be redundant (e.g. the same measurement in both feet

and meters, or the repetitiveness of images presented as pixels), then it can be transformed into a reduced set of features (also named a feature vector). Determining a subset of the initial features is called feature selection. The selected features are expected to contain the relevant information from the input data, so that the desired task can be performed by using this reduced representation instead of the complete initial data [8].

A major issue in any pattern classification system is the extraction of proper features that effectively differentiate various patterns. In the last few decades, various feature extraction schemes were developed. Usually in feature extraction, the visual information of an image is analyzed in order to produce features such as shape, texture and color [9].

3.4 k- Nearest Neighbours

Classification system consists of database that contains predefined patterns that compares with detected object to classify in to proper category. Image classification is an important and challenging task in various application domains, including biomedical imaging, biometry, video surveillance, vehicle navigation, industrial visual inspection, robot navigation, and remote sensing [10]. Two types of classification are supervised and unsupervised classification [11].

k-NN algorithm is one of the simplest classification algorithm and it is one of the most used learning algorithms. k-NN is a non-parametric, lazy learning algorithm. Its purpose is to use a database in which the data points are separated into several classes to predict the classification of a new sample point. k-NN is a very simple algorithm used to solve classification problems. k is the number of neighbors in k-NN [12].

The simplest, most used instance-based learning algorithm is the k-NN algorithm. The k-NN assumes that all instances are points in some n-dimensional space and defines neighbors in terms of distance (usually Euclidean in R-space). Using the second property, the k-NN classification rule is to assign to a test sample the majority category label of its k nearest training samples. In practice, k is usually chosen to be odd, so as to avoid ties. The $k = 1$ rule is generally called the nearest-neighbor classification rule [13]. The Euclidean distance is used to determine the distance between train feature and test feature. The classification process by k-NN is shown in Figure 3[14].

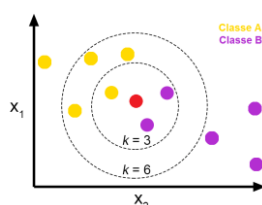


Figure 3. k-NN classification algorithm[14]

4. IMPLEMENTATION PROCESS

The proposed system have mainly three steps such as: collecting hand gestures (Imageset), training

dataset and recognition the hand gesture. The implementation process of the proposed system is considered mainly two conditions as shown in Figure 4. In the first condition, only Gaussian filter is considered to reduce noise. The hand gesture image is captured by WebCam and converted to grayscale. And then the noise of the grayscale image is reduced by using Gaussian filter. After that the output of the filter is recognized with trained dataset. If the gesture image is matched with trained data, the corresponding text and speech are appeared on result test box and the built-in speaker respectively. In the second condition, both bilateral and Gaussian filters are considered to reduce noise. The primary goal of the bilateral filter is to denoise the imaging on original frame and to produce sharp image.

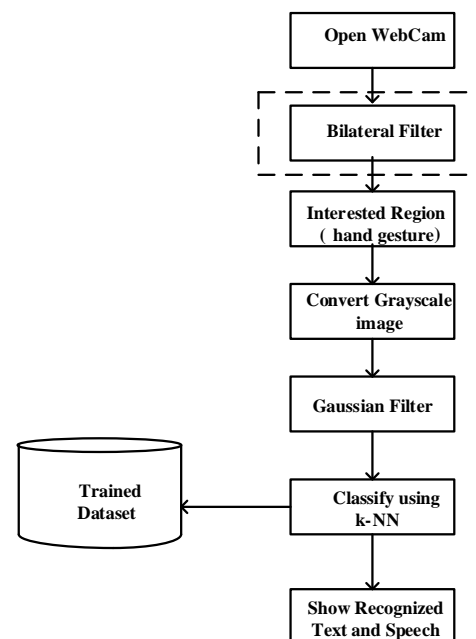


Fig 4. The Implementation Process of the proposed system

4.1 Image Set

The input video stream is fed to computer vision. In first case, the noise of whole frame is not reduced by bilateral filter. The noise of the original frame of WebCam is reduced by bilateral filter. The captured image in rectangular box of interested region is detected by contour and convex hull. And then it is converted to grayscale image and smoothing the gray scale image by using Gaussian filter. The imageset can be obtained by collecting hand gesture image. The interested region is bounded by rectangular box that is shown in Figure 5. Then, background subtraction technique is used that is shown in Figure 6. After background subtraction, image box is appeared.

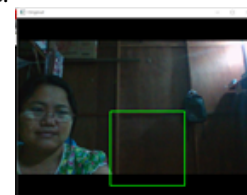


Fig 5. Interested Region (Green Rectangular Box)

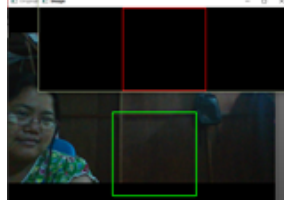


Fig 6. After Background subtraction

In this paper, the hand gesture images from 'ဝ' to 'ခ' are based on Myanmar Sign Language by Mary Chapman School for the Deaf in Yangon. The gesture image for each alphabet and unknown sign are collected to get imageset. And so, there are totally 320 gestures in the imageset. The hand region is detected by contour and convex hull and it is converted grayscale image and then the smoothing gesture image is get using Gaussian filter. This is shown in Figure 7. Figure 8 is that Gaussian filter for reduce noise and also the bilateral filter is used for the original whole frame.

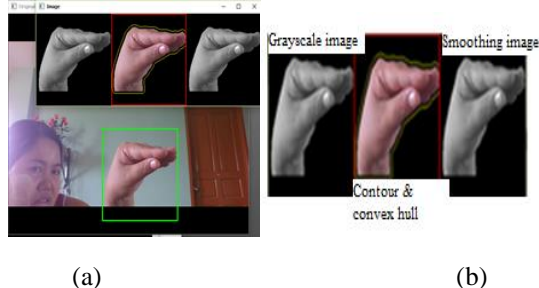


Fig 7. Hand Gesture for ဂ using only Gaussian Filter (a) The whole view for ဂ (b) Image box for ဂ

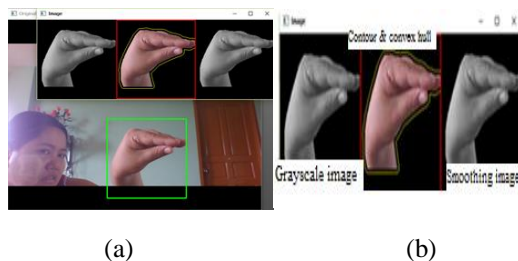


Fig 8. Hand Gesture for ဂ using both bilateral and Gaussian Filters (a) The whole view for ဂ (b) Image box for ဂ

The imageset can be obtained by collecting hand gesture image as shown in Figure 9 and Figure 10. Image sets are created in both cases at the same time and same place.



Fig 9. Image set for ဂ using only Gaussian filter

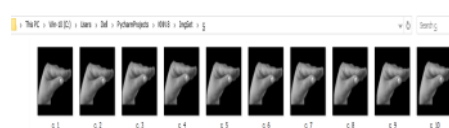


Fig 10. Image set for ဂ using both bilateral and Gaussian filters

4.2 Dataset

The collected hand gesture image set is trained with corresponding pixels values and each hand gesture is labelled by corresponding text and speech. The result of training image set is trained data set as shown in Figure 11.

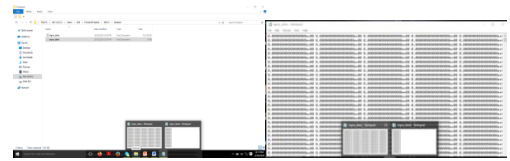


Fig 11. Dataset for this system

4.3 Real-Time Testing

In first case, Open the WebCam and not reduce the noise of whole frame and create the interested region and then background subtraction is used. Then, the detected hand gesture is converted the grayscale image and denoised. Finally, the hand gesture is recognized by train dataset using k-NN classifier and the corresponding output text is shown from result text box and the built-in speaker out speech. In this paper, the value of k is 1. In second case, the noise of whole frame is reduced by bilateral filter.

5. EXPERIMENTAL RESULTS

Real-time testing can be started after implementing the trained dataset. When Webcam is opened, the interested region and result test box are shown in Figure 11.

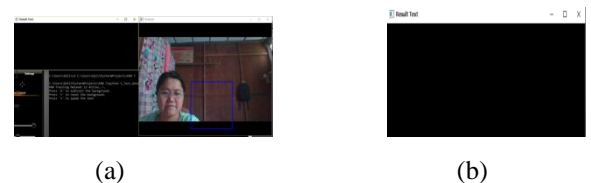


Fig 11. Starting Condition of Recognition System (a) Rectangular Box for Interested Region (b) Result Test Box

After using background subtraction, all image views is appeared as in Figure 12. In second case, bilateral filter is used to reduce the noise of overall original frame.

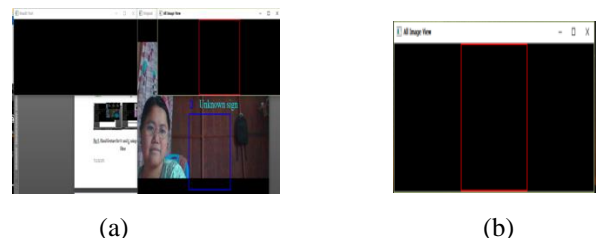


Fig 12. Steps for real-time testing (a) After Background Subtraction (b) All Image Views

As soon as hand gesture has captured by WebCam, the captured image is converted to grayscale and reduced noise by Gaussian filter. After that the denoising image is recognized by pretrained dataset using k-NN classifier with the value of k=1. If the gesture

image is matched with one of trained data, the corresponding text and speech are appeared in result test box and the built-in speaker respectively. In this papers, hand gesture image recognition is processed with only Gaussian filter and both bilateral and Gaussian filters in order to compare the performance results. In both case, the hand gestures are tested in ten times for each alphabet. The isolated results are described in Figure 13 and Figure 14.

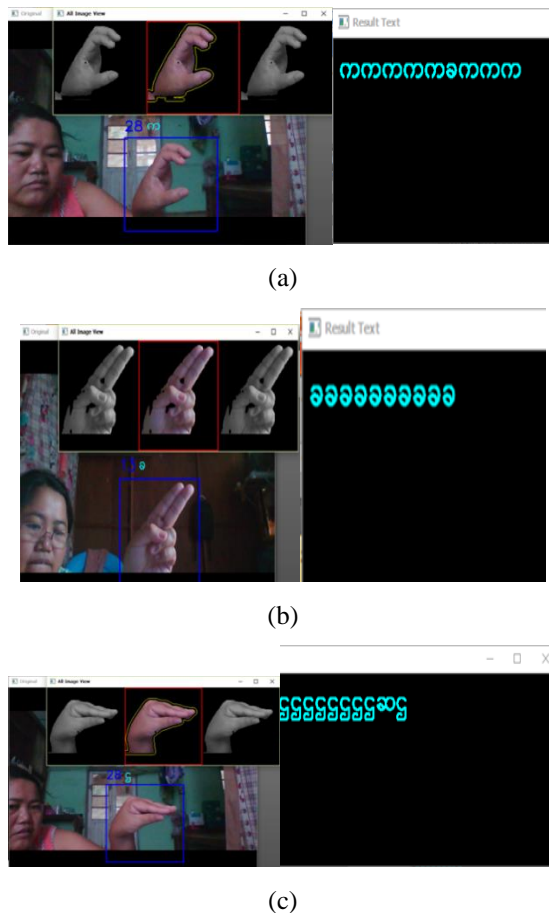


Fig 13.The Testing Result with only Gaussian Filter (a) For Alphabet က (b) For Alphabet ခ (c) For Alphabet ဂ

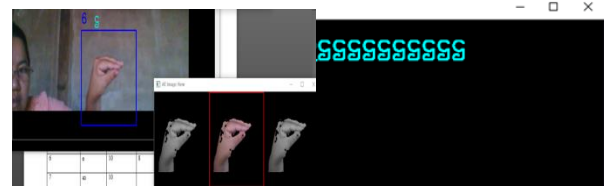
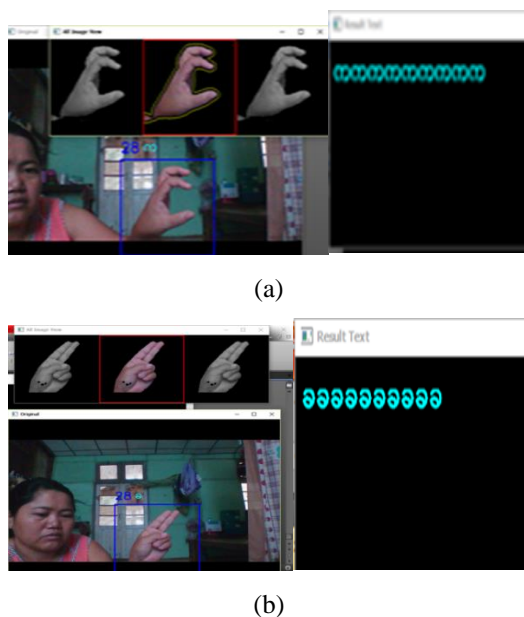


Fig 14.The Testing Result with both Bilateral and Gaussian Filter (a) For Alphabet က (b) For Alphabet ခ (c) For Alphabet ဂ

The recognition accuracy of this system is shown in Table 1.

Table 1 Recognition Accuracy for 31 Static Alphabets

No	Alphabets	Testing Times	Case (1)		Case (2)	
			Corrected times	% error	Corrected times	% error
1	က	10	9	10%	10	0%
2	ခ	10	10	0%	10	0%
3	ဂ	10	5	50%	9	10%
4	ဃ	10	9	10%	10	0%
5	င	10	10	0%	10	0%
6	စ	10	10	0%	10	0%
7	ဆ	10	9	10%	9	10%
8	ည	10	7	30%	10	0%
9	ဋ	10	10	0%	10	0%
10	ဌ	10	9	20%	10	0%
11	ဍ	10	10	0%	10	0%
12	ဎ	10	8	20%	8	20%
13	ဏ	10	10	0%	10	0%
14	တ	10	10	0%	10	0%
15	ထ	10	8	20%	9	10%
16	ဒ	10	8	20%	9	10%
17	ဓ	10	9	10%	10	0%
18	န	10	7	30%	7	30%
19	ပ	10	8	20%	9	10%
20	ဖ	10	7	30%	9	10%
21	ဗ	10	7	30%	10	0%
22	ဘ	10	6	40%	8	20%
23	မ	10	5	50%	7	30%
24	ယ	10	9	10%	10	0%
25	ရ	10	7	30%	10	0%
26	လ	10	9	10%	10	0%
27	ဝ	10	10	0%	10	0%
28	သ	10	10	0%	10	0%
29	ဟ	10	10	0%	10	0%

30	င	10	3	70%	5	50%
31	အ	10	10	0%	10	0%
				17%		7%

Figure 15 shows the results k-NN classifier using only Gaussian filter and using both bilateral and Gaussian filters.

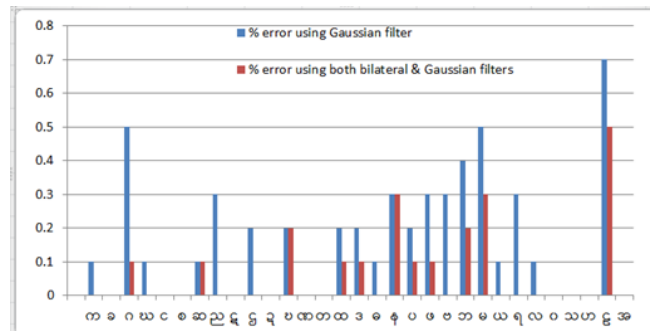


Fig 15. Recognition Accuracy of the Proposed System using only Gaussian filter and both Bilateral and Gaussian Filters

According to the experimental results, the performance accuracy is 93% by using both bilateral and Gaussian filters, whereas that is 83% by using only Gaussian filter. Alphabet 'ခ' is misclassified with 'စ', alphabet 'ဆ' is misclassified with 'ဝ', alphabet 'င' is misclassified with 'အ', alphabet 'ရ' is misclassified with 'ဝ', alphabet 'န' is misclassified with 'စ', alphabet 'လ' is misclassified with 'င' and alphabet 'တ' is misclassified with 'ဘ' because these two hand gestures representation are similarities in shape.

6. CONCLUSIONS

The proposed system can handle different types of Myanmar alphabet signs in a common vision-based platform. The main focuses of this system is that image processing is applied as a tool for the conversion of hand gesture into text and speech in Myanmar alphabet. As there are many similar gestures in MSL, there is misclassification in recognition system.

The main hypothesis of this paper is to demonstrate that the better performance of MSL recognition system can achieve by using both bilateral and Gaussian filters. This research work can also be extended to recognize dynamic hand gestures (ခ and ချ), Myanmar words and sentences using video processing.

ACKNOWLEDGEMENT

The authors wish to express special thanks to all the teachers from the Department of Electronic Engineering, Technological University (Hmawbi), for their kind help, encouragement, true-line guidance, and support. The authors would like to express their thanks to all persons who have contributed directly or indirectly towards the successful completion of this paper. And also express thanks to all persons whom will concern to

support in papering this research and for their technical feedback on important issues.

REFERENCES

- [1] Fitrah Maharani Humaira "Real Time SIBI Sign Language Recognition based on K-Nearest Neighbor" Proceeding of EECSE 2018, Malang - Indonesia, 16-18 Oct 2018
- [2] Muhammad Aminur Rahaman, Mahmood Jasim "Real-Time Computer Vision-Based Bengali Sign Language Recognition" 17th Int'l Conf. on Computer and Information Technology, 22-23 December 2014, 978-1-4799-6288-4/14/\$31.00 ©2014 IEEE
- [3] Priyanka Lokhande, "Data Glove For Sign Language Recognition System" International Journal of Computer Applications (0975 – 8887) National Conference on Emerging Trends in Advanced Communication Technologies (NCETACT-2015)
- [4] https://en.wikipedia.org/wiki/Foreground_detection
- [5] <https://courses.cs.washington.edu>
- [6] [https://www.mathworks.com/matlabcentral/Gaussian filter](https://www.mathworks.com/matlabcentral/Gaussian_filter)
- [7] https://en.Wikipedia.org/wiki/Bilateral_filter
- [8] https://en.wikipedia.org/wiki/Feature_extraction
- [9] Theory for feature extraction
- [10] Pooja Kamavisdar, "A Survey on Image Classification Approaches and Techniques" International Journal of Advanced Research in Computer and Communication Engineering Vol. 2, Issue 1, January 2013
- [11] Image Processing and Analysis Using MATLAB, Dr. Nay Zar Aung, Ph.D (Mechatronics), HIT
- [12] <http://advantages and disadvantages of knn.html>
- [13] CS 478 - Machine Learning, Instance Based Learning (Adapted from various sources)
- [14] <https://blog.usejournal.com/a-quick-introduction-to-k-nearest-neighbor-algorithm-62214cea29c7>

TRAJECTORY TRACKING CONTROL SYSTEM OF MOBILE ROBOT

Hnin Yu Wai⁽¹⁾, Yin Yin Soe⁽²⁾

^{(1), (2)} Department of Electronic Engineering, Technological University (Thanlyin), Myanmar

¹hninw3234@gmail.com

²dr.yin2soe@gmail.com

ABSTRACT: This paper presents the trajectory tracking control system of wheeled mobile robot (WMR). At first, the kinematic model of the robot is presented which is the base of control law. And then, the proportional (P) controller and proportional-integral controller (PI) are used for controlling left and right wheel velocity of robot such that the tracking errors are minimized between the robot and user defined trajectory. When the (P) controller only is used the trajectory produced the appropriate result to reach the desired position. Such that, the (I) controller is added to improve the result of desired position. Experimental results with MATLAB simulation are provided to analysis the control algorithm of wheeled mobile robot.

KEYWORDS: *Wheeled mobile robot (WMR), (P) Controller, (PI) Controller, Trajectory Tracking, MATLAB*

1. INTRODUCTION

Mobile robots are found in many places such as indoor environments in cleaning large building, transportation industry and service, and outdoor environments in agriculture, forest, firefighting and military [1]. Most of them have focused on trajectory tracking control system of mobile robot to follow a desired trajectory. Robot control with non-holonomic constraints on a predefined path is an essential task in mobile robotics application [2]. The control problem of mobile robots caused by free motion of wheels in position and orientation, therefore control signals under the non-holonomic kinematics constraints are needed [3]. The motion of this robot is considered by using its kinematics model because the control problem is easier to solve. There are many control algorithms to control the trajectory tracking of mobile robot from the start to the end position. Wu, et al. (2001) presented a PD controller that the velocity is the control objective to control a guidance mobile robot [4]. Vieira, et al. (2004) proposed the position and orientation estimation method of a two-wheeled differentially driven non-holonomic mobile robot [5]. PID controllers are widely used and there are various types of process to regulate PID controllers [6]. Hazry, et al. (2006) proposed new development for proportional parameter estimation in mobile robot for stable tracking control system [7]. Desa, et al. (2015) presented the application of PI and model predictive control of mobile robot trajectory tracking [8]. Kumar et al. (2018) proposed tracking of a PID driven differential drive mobile robot [9]. Many

applications involve tracking a desired trajectory or reaching a set point require the mobile robot to be able to accurately define its position and orientation during motion.

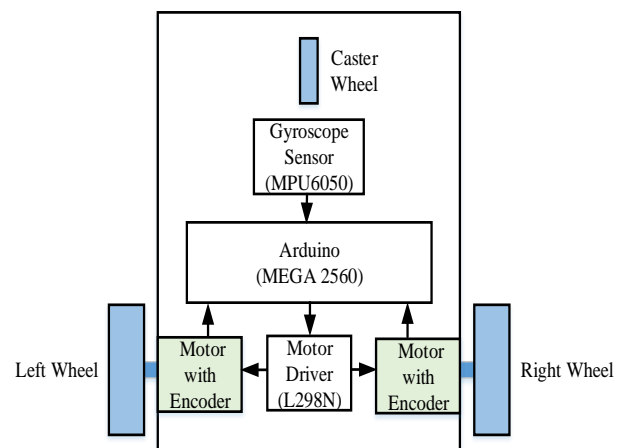


Fig 1. Wheeled mobile robot layout and system block

In this system, wheeled mobile robot layout and system block is as shown in Fig 1. Gyroscope is used to receive orientation angle from the rotation about z-axis. Arduino Mega 2560 board is used in the controller section. The L298 motor driver is used to drive the two DC motors and motor angular positions are received from two encoders. The two wheels are mounted on those motor's shafts to move mobile robot. In technical content, a kinematic model and solving of trajectory tracking problem are presented. The proportional (P) controller and proportional-integral controller (PI) are used for controlling WMR. Trajectory tracking of WMR for moving one-point is considered in obstacle free place. The experimental tests are used and the simulation results are proposed that are seen to show better trajectory tracking.

This paper is organized as follows: section II presents the kinematic model of the WMR and control system. In section III experimental tests and results of one-point tracking. In section IV conclusions are presented.

2. ROBOT MODEL AND CONTROL SYSTEM

2.1 Kinematic Model

Kinematic model of the WMR is considered as a simple illustration of mobile robot as shown in Fig 2. The two rear wheels of the robot are controlled by the two independent DC motors, and a front castor wheel is

used to balance the robot. The position of the robot is specified by (x, y) denote at point O (center of axis of the driven wheels), v is the linear velocity of the center body and θ is the orientation angle of the robot in the world coordinate frame which is received from gyroscope. Velocities of the left and right wheel are denoted by v_L and v_R .

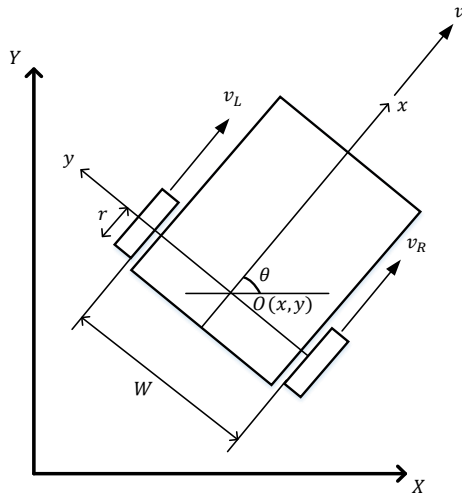


Fig 2. Kinematic model of WMR.

The kinematic model of motion equations in the world frame can be represented as follows [10]:

$$\dot{x} = v \cos \theta \quad (1)$$

$$\dot{y} = v \sin \theta \quad (2)$$

$$\dot{\theta} = \frac{\Delta v}{W} \quad (3)$$

The position of robot is computed by using the following equations. Where r is the radius of wheel, β_L and β_R are rotation angles of left and right motor.

$$v_L = r \frac{d\beta_L}{dt} \quad (4)$$

$$v_R = r \frac{d\beta_R}{dt} \quad (5)$$

$$v = \frac{v_R + v_L}{2} \quad (6)$$

$$x = \int v \cos \theta dt \quad (7)$$

$$y = \int v \sin \theta dt \quad (8)$$

2.2 Control System

The PID controller is a feedback closed loop control system. The three terms are called proportional (P), integral (I), and derivative (D), and (P) term acts on the current error, (I) term acts on the previous error and (D) term acts future error based on the rate of change of error between the current and previous error so as to determine an appropriate control signal to reduce the error. These three outputs are shown in Fig 3.

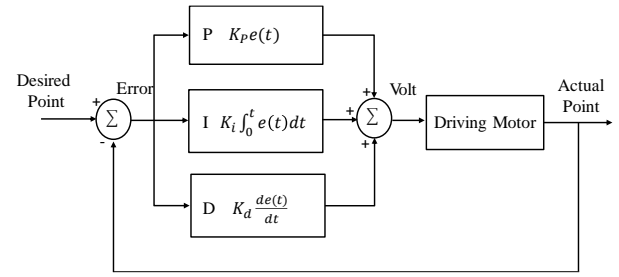


Fig 3. Block diagram of PID controller

In proposed system, proportional (P) and proportional-integral (PI) controller are consist of tuning parameters (K_P) and (K_I) those represent the gains of the present and previous error. The goals of the (P) and (PI) controller are to control the motor in such a way that the robot reaches the desired position x^* and y^* .

The proportional (P) and proportional-integral (PI) controller are taken as follows:

$$v^* = K_P e(t) \quad (9)$$

$$v^* = K_I \int e(t) dt \quad (10)$$

Following trajectory, desired angle and error distance are calculated as follows:

$$\theta^* = \tan^{-1} \frac{y^* - y}{x^* - x} \quad (11)$$

$$e = \sqrt{(x^* - x)^2 + (y^* - y)^2} \quad (12)$$

The desired velocities of right and left motor are computed as follows:

$$v_R^* = \left(\frac{2 * v^* + \left(W * \frac{d\theta^*}{dt} \right)}{2} \right) \quad (13)$$

$$v_L^* = (2 * v^*) - v_R^* \quad (14)$$

Where W is distance between the two wheels and v^* is desired signal.

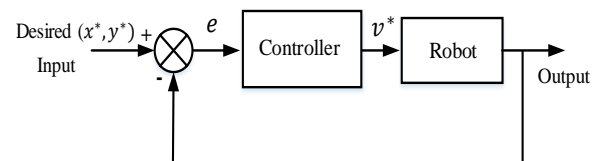


Fig 4. Block diagram of control system

In Fig 4, it is the presented block diagram of control system where (P) and (PI) controller are used. This feedback system ensures that the robot reaches to a point, it compares the actual (x, y) position of the robot with desired (x^*, y^*) position. It is the error value of difference between the desired and actual position of the robot. The input of the controller is an error value and the output is desired signal to drive the motor. The desired velocities of right and left motor are calculated by using equations (13) and (14), such that robot moved to user defined position. Model of a wheeled mobile robot is illustrated in Fig 5.

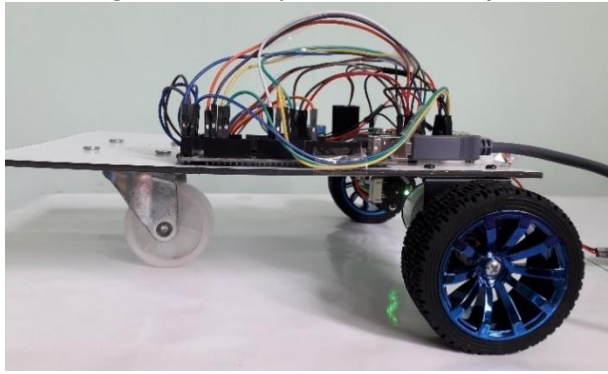


Fig 5. Model of WMR

3. EXPERIMENTAL RESULTS

3.1 One-Point Tracking

In this section, (P) and (PI) controller are used to follow one-point trajectory of a wheeled mobile robot. The experimental results of both controllers can be compared.

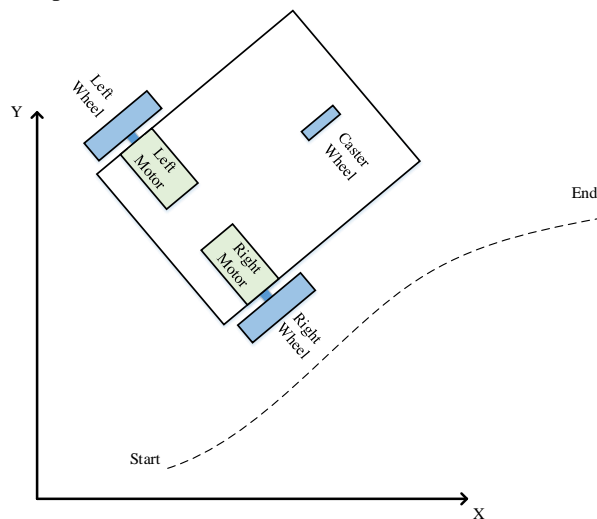


Fig 6. Diagram of WMR trajectory tracking

In this experimental tests, a start position $(x_{start}, y_{start}) = (0, 0)$ and a desired position $(x_{desired}, y_{desired}) = (50, 50)$ are considered. In Fig 7. (a) and 7. (b), tracking comparison by using controllers along X-axis and Y-axis are shown with the following figures.

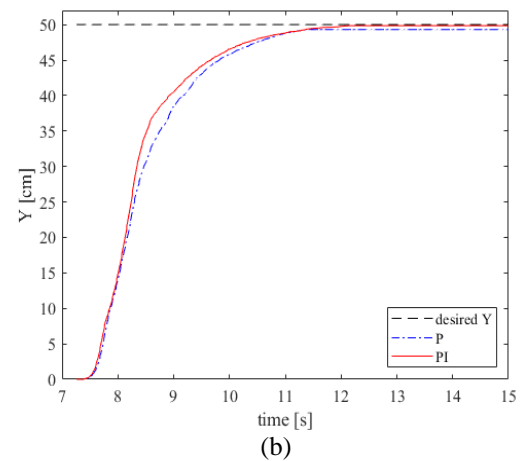
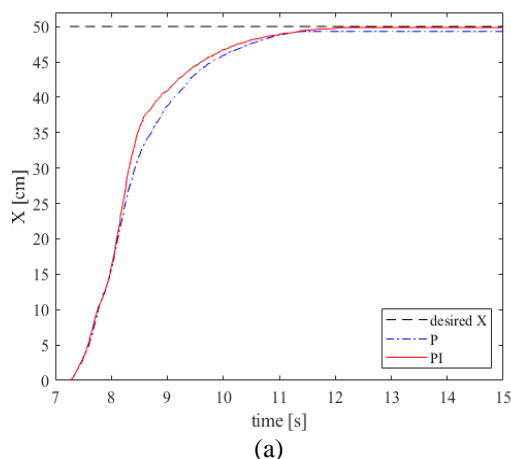
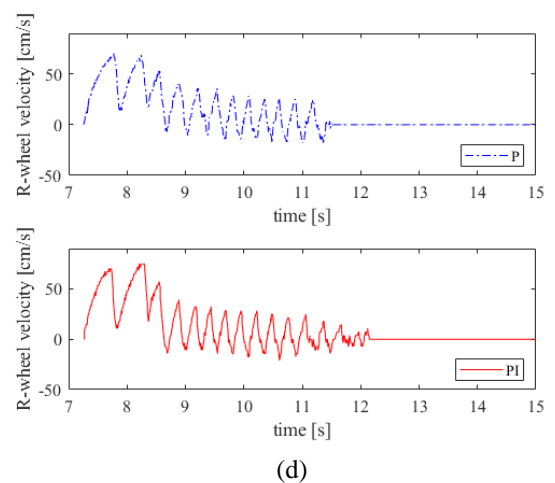
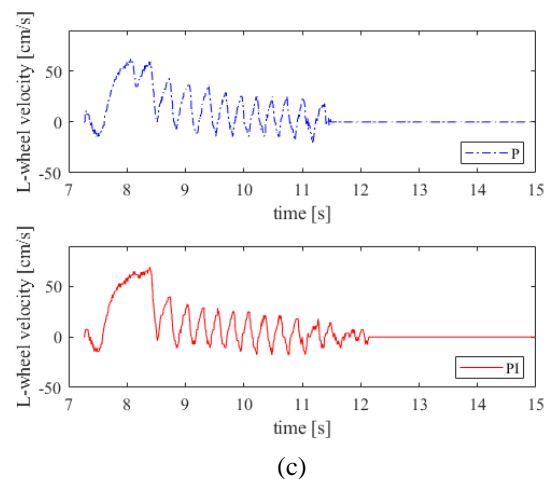


Fig 7. (a) Results of one-point tracking based on P and PI controller along X-axis

(b) Results of one-point tracking based on P and PI controller along Y-axis

In Fig 7. (c) and 7. (d), left and right wheel velocity comparison by using controllers are shown with the following figures.

Fig 7. (c) Left wheel velocity based on P and PI controller
(d) Right wheel velocity based on P and PI controller

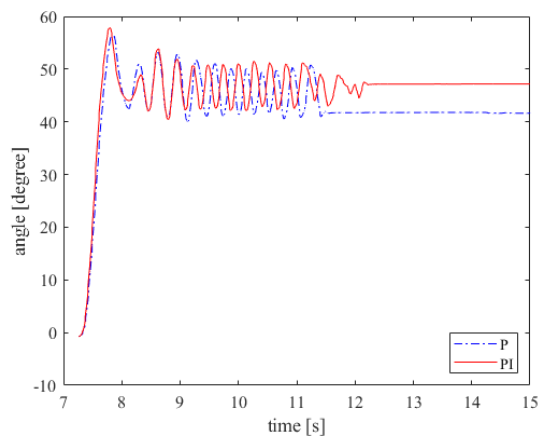
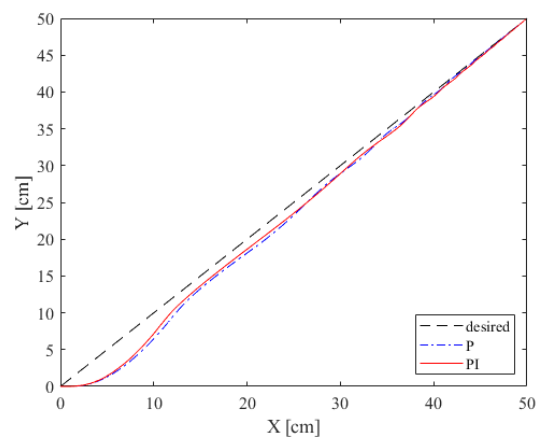
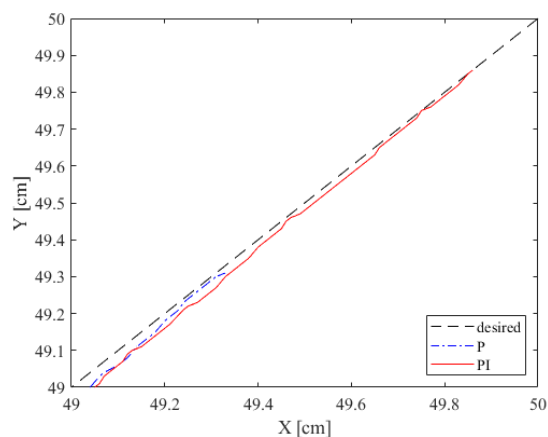


Fig 7. (e) Orientation angle (θ) of the mobile robot based on P and PI controller

In Fig 7. (f) and 7. (g), results of trajectory condition on the X-Y plane comparison by using controllers are shown with the following figures.



(f)



(g)

Fig 7. (f) Trajectory of the mobile robot on the X-Y plane based on P and PI controller
(g) Results of trajectory between (49cm and 50 cm) on the X-Y plane based on P and PI controller

From the above experiments, parameters and comparison results of the mobile robot for trajectory tracking with (P) and (PI) controller are illustrated in table 1. The experimental results of (P) controller cannot

provided the desired condition. It is shown that the (PI) controller which provided complete approximately the desired condition for one-point trajectory system.

Table 1. Parameters and experimental results for one-point tracking

Controller	Parameter K_P	Parameter K_i	Result % (50, 50)
P	1.0	-	98.62%
PI	1.0	0.001	99.72%

Table 2. Effect of PID parameter [11]

Closed Loop Response	Rise Time	Over-shoot	Settling Time	Steady-State Error
KP	De-crease	In-crease	Small Increase	De-crease
KI	De-crease	In-crease	Increase	Large decrease
KD	Small De-crease	De-crease	Decrease	Minor change

The proportional (P) controller is used to decrease the steady state error of the system. The proportional- integral (PI) controller is used to eliminate the steady state resulting error from (P) controller. The K_P and K_i parameters are adjusted to obtain its optimal values for the desired control response. Effect of PID parameter is illustrated in table 2. In this experiments mobile robot may oscillate due to noise of the measured sensor errors from external sources. Therefore, filtering to the sensor reading should be used to achieve relatively accurate estimation of robot orientation angle.

4. CONCLUSIONS

In this proposed system, one-point trajectory tracking of WMR is enabled by using P and PI controller. It was good enough for basic tracking problem. A trajectory depends on the accuracy of DC motor rotation and controller. The proposed (P) and (PI) controller were compared with the experimental results, the (PI) controller achieved good result for desired trajectory tracking. This proposed controller has shown good performance to control the robot but it still has little steady state error and not accurate 100%. Moreover, by using another controller, the robot can move to reach the desired positions with optimal performance and zero level error.

ACKNOWLEDGMENT

The author wishes to express grateful thanks to Dr. Theingi, Rector of Technological University (Thanlyin). The author would like to acknowledge Dr. Aye Mya Win, Professor and Head, Department of Electronic Engineering, Technological University (Thanlyin), for her valuable guidance, and encouragement. The author wishes to express the deepest thanks and gratitude to her supervisor Dr. Yin Yin Soe, Associate Professor, Department of Electronic Engineering, Technological University (Thanlyin) for her close guidance, accomplished supervision, help, support and edition during this research. The author particularly wishes to acknowledge all the teachers from the Electronic Research and Seminar Room, Technological University (Thanlyin).

REFERENCES

- [1] G. Mester, "Applications of Mobile Robots," 7th International Conference on Food, April 2006.
- [2] C.C. Wit and R. Roskam. "Path Following of a 2-DOF Wheeled Mobile Robot Under Path and Input Torque Constraints," IEEE Transaction on Robotics and Automation, vol. 2, no. 1, pp. 1142-1147, 1991,
- [3] M.J. Mohamed, M.Y. Abbas, "Design of Fuzzy PID Controller for Trajectory Tracking of Mobile Robot," Engineering and Technology Journal, vol. 36, Part A, No. 1, pp. 100-110, 2018.
- [4] S.F. Wu, J.S. Mei and P.Y. Niu, "Path Guide and Control of Guided Wheeled Mobile Robot," Control Engineering, vol. 9, no. 3, pp. 29-31, 2001.
- [5] F.C. Vieira, A.A.D. Medeiros, P.J. Alsina and A.P. Araujo, "Position and Orientation Control of a Two-wheeled Differentially Driven Nonholonomic Mobile Robot," 1th International Conference on Information in Coontrol, Automation and Robotics, August 25-28, 2004.
- [6] P. Mhaskar, N. H. El-Farra and P. D. Christofidest, "A Method for PID Controller Tuning Using Nonlinear Control Techniques," Proceedings of the American Control Conference, pp. 2925-2930, 2004.
- [7] H. Desa, and M. Sugisaka, "Proportional Control for Trajectory Tracking of a Wheeled Mobile Robot," SICE-ICASE International Joint Conference, pp. 5283 – 5285, Oct 18-21, 2006.
- [8] M. Manel and B. Faouzi, "Trajectory Tracking of Two Wheeled Mobile Robot," 6th International Conference on Modeling, Simulation, and Applied Optimization (ICMSAO), pp. 1-6, May, 2015.
- [9] U. Dinesh Kumar, M. Nisha and Mathivanan, "Tracking of a PID Driven Differential Drive Mobile Robot," International Journal of Mechatronics and Computer Technology (IJMEC), vol. 8 (27), pp. 3690-3704, Jan, 2018,
- [10] P. Corke, "Robotics, Vision and Control: Fundamental Algorithm in Matlab," Springer, 2011.
- [11] J. Zhong, "PID Controller Tuning: A Short Tutorial," Mechanical Engineering, Purdue University Spring, 2006.

- [12] E.O.C. Torres, "Traction Modeling and Control of a Differential Mobile Robot to Avoid Wheel Slip," Master's thesis, Oklahoma State University, 2013.
- [13] N. Leena and K.K. Saju, "Modeling and Trajectory Tracking of Wheeled Mobile Robots," Procedia Tech, vol. 24, pp. 538-545, 2016.

Supervisory Control and Data Acquisition Based Air Conditioning System

Dr. Thida Aung⁽¹⁾, Ko Ko Zaw⁽²⁾

⁽¹⁾Technological University (Lashio), Myanmar

⁽²⁾West Yangon Technological University, Myanmar

Email: thidaaung@tulashio.edu.mm

koko.ttu.meecl@gmail.com

ABSTRACT: This paper, Supervisory Control and Data Acquisition (SCADA) based Air Conditioning System, illustrates the application of SCADA devices not only for industry but also for the home. As a SCADA master unit, the personal computer provides a graphical user interface (GUI) and automatically regulates the managed air conditioning system in response to sensor inputs. The AT89SC51 microcontroller is applied for a Remote Telemetry Unit (RTU). This controller serves as a local collection point for gathering reports from temperature sensors and delivering commands to control relays for the actuators in both indoor and outdoor unit. The communications network, RS 232 protocol connects the SCADA master unit to the RTUs of the system. The engineering software tools, Visual Basic and Assembly language, are used to develop GUI and communication protocol between personal computer and microcontroller.

KEYWORDS: *Supervisory Control and Data Acquisition (SCADA), Graphical User Interface (GUI), AT89SC51, Remote Telemetry Unit (RTU), Visual Basic*

1. INTRODUCTION

Supervisory Control and Data Acquisition (SCADA) is a real-time industrial process control system used to centrally monitor and control remote or local industrial equipment such as motors, valves, pumps, relays, sensors, etc. SCADA is the combination of telemetry and Data Acquisition [1]. Previously without SCADA software, an industrial process was entirely controlled by PLC, CNC, PID & micro controllers having programmed in certain languages or codes. These codes were either written in assembly language or relay logic without any true animation that would explain the process running. It is always easy to understand the status of the process if it is shown with some animations rather than written codes. Hence SCADA software came to existence with some exclusive features [2] and it became internal part of automation system. SCADA is not only hardware but also software. It's a concept. It's a system as a combination of special hardware, software and protocols. SCADA is used to control chemical plant processes, oil and gas pipelines, electrical generation and transmission equipment, manufacturing facilities, water purification and distribution infrastructure, etc. For

example, in a SCADA system, a PLC can be used to control the flow of cooling water as part of an industrial process. At the same time the supervisor can use the Host control function to set the temperature for the flow of water. It can also have alarms and can record the flow of water temperature and report back to supervisor. The RTUs and PLCs are responsible for data collection such as meter readings, equipment status, etc and communicate back to the SCADA system. This data can be stored in a database for later analysis or monitored by a supervisor to take appropriate actions if required.

SCADA systems typically implement a distributed database, commonly referred to as a tag database, which contains data elements called tags or points. A point represents a single input or output value monitored or controlled by the system. Points can be either "hard" or "soft". A hard point is representative of an actual input or output connected to the system, while a soft point represents the result of logic and math operations applied to other hard and soft points [3].

The overall block diagram of SCADA based Air Conditioning System is shown in Fig. 1. Air conditioning system is designed and constructed by using 8051 microcontroller which also interfaces with Personal Computer based on Visual Basic (VB) software. The air conditioning system is controlled from Personal Computer with the help of 8051, and this type of data acquisition system is so-called SCADA system, contrary to the one constructed in market by using different type algorithm. Controlling of environment temperature, heat, coldness process, speed of electric fan is done by PC control according to the database and user's settings. All of the parameter such as temperature, electric fan control and louver position can be controlled in GUI of personal computer.

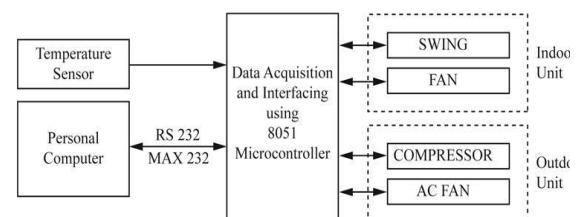


Fig.1 Overall Block Diagram of SCADA based Air Conditioning System

2. HARDWARE DESIGN SCHEME

The proposed air conditioning system consists of temperature sensor, analog to digital converter (ADC0809), microcontroller AT89S51, RS 232 serial communication, MAX 232, stepper motor and asynchronous AC motor.

2.1 Temperature Sensor

The temperature sensor is assembled one with various parts and thermistor devices consistent with the specified applications. Its electric characteristics are an equivalent as those of thermistor devices. Variable sorts of sensor are often utilized for detecting or controlling temperature because its operating temperature range is wide from -50°C to $+300^{\circ}\text{C}$. Centigrade sensor is out there in accordance with the applications like measurements of liquid, atmosphere and surface temperature. External temperature sensors need to be ready to withstand moisture, heat, frost, road salt and high washing. Moisture could slowly creep from critical parts like material junctions up to the sensor head and cause it to fail. The NTC are often protected as long as it's a part of a totally sealed system. For this reason, cabled sensors are recommended, in order that the connector isn't located near any moisture. If the connector is molded directly onto the external temperature sensor, the connector must be absolutely watertight. No moisture must get to the sensor before the mounting of the connector. The junction of the plastic to the metal contacts can never be absolutely moisture-tight. The NTC should be completely encapsulated and bonded to the cable [4]. The temperature sensor for air conditioning system is shown in Fig. 2.



Fig. 2 Temperature Sensor

2.2 Analog to Digital Converter (ADC0809)

The ADC0809 data acquisition component is a monolithic CMOS device with an 8-bit analog-to-digital converter, 8-channel multiplexer and microprocessor compatible control logic. The 8-bit A/D converter uses successive approximation as the conversion technique. The converter features a high impedance chopper stabilized comparator, a 256R voltage divider with analog switch tree and a successive approximation register. The 8-channel multiplexer can directly access any of 8-single-ended analog signals.

The device eliminates the need for external zero and full-scale adjustments. Easy interfacing to microprocessors is provided by the latched and decoded multiplexer address inputs and latched TTL outputs. The

design of the ADC0809 has been optimized by incorporating the most desirable aspects of several A/D conversion techniques. The ADC0809 offers high speed, high accuracy, minimal temperature dependence, excellent long-term accuracy and repeatability, and consumes minimal power. These features make this device ideally suited to applications from process and machine control to consumer and automotive applications. The ADC0809 operates ratio metrically or with 5 V DC or analog span adjusted voltage reference with 0V to 5V input range. It is 8-channel multiplexer with address logic and standard hermetic or molded 28-pin DIP package [5]. It is equivalent to MM74C949-1.

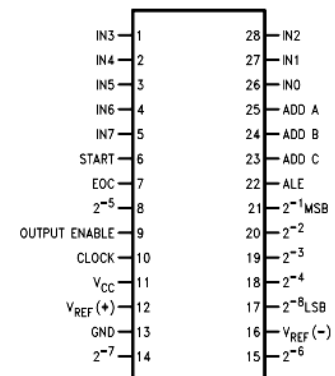


Fig. 3 Pin Diagram of ADC0809 Converter

2.3 Microcontroller AT89S51

The AT89S51 is a low-power, high-performance CMOS 8-bit microcontroller with 4k bytes of In-System Programmable Flash memory. The device is manufactured by using Atmel's high-density nonvolatile memory technology and is compatible with the industry-standard 80C51 instruction set and pin out. The on-chip Flash allows the program memory to be reprogrammed in-system or by a conventional nonvolatile memory programmer. By combining a versatile 8-bit CPU with In-System Programmable Flash on a monolithic chip, the Atmel AT89S51 is a powerful microcontroller, which provides a highly flexible and cost-effective solution to many embedded control applications.

The AT89S51 provides the following standard features: 4k bytes of Flash, 128 bytes of RAM, 32 I/O lines, watchdog timer, two data pointers, two 16-bit timer/counters, a five-vector two-level interrupt architecture, a full duplex serial port, on-chip oscillator, and clock circuitry.

In addition, the AT89S51 is designed with static logic for operation down to zero frequency and supports two software selectable power saving modes. The idle mode stops the CPU while allowing the RAM, timer/counters, serial port, and interrupt system to continue functioning. The power-down mode saves the RAM contents but freezes the oscillator, disabling all other chip functions until the next external interrupt or hardware reset [6].

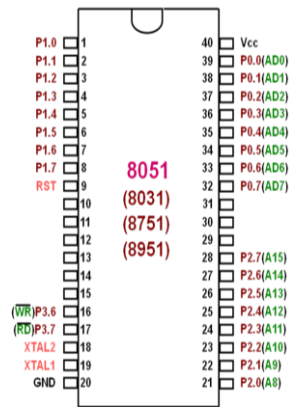


Fig. 4 Pin Configuration of AT89S51 Microcontroller

3. IMPLEMENTATION OF THE SYSTEM

In order to meet the software requirements of SCADA system, Visual Basic programming language is used for Graphical User Interface (GUI) in PC, the master unit of a SCADA and assembly language is used for Remote Telemetry Unit (RTU). For hardware portion, temperature sensing circuit with ADC to interface AT89S51 microcontroller, stepper motor driver circuit, relay driver circuit for actuators and RS 232 interface circuit using MAX232 IC are constructed and tested step by step.

3.1 Software Implementation for Communication

The VB's software is designed to operate air conditional control system. VB's window is made up of boxes. Each box contains information related to configurable parameters needed for configuring. For the PC application, a source code VB file is used. The VB file has multiple configurable items in it. Each item is broken up into sections relating to the specific area for which the code is used. The section contained in VB files are: RS232, COM port setting, sensor data and display section. PC's serial data acquisition interfaces require the sending and receiving of ASCII data to operate. To communicate with the serial port using visual basic, the MSComm control must be utilized to allow serial data transfer via a serial port.

3.2 User Interface Window

In this research, the program is constructed to control air conditional system. This program is arranged step by step or procedurally and it consists of a series of steps that take place one after another. The programmer decides the condition under which a procedure takes place, how often it takes place and when the program stops. This program has been implemented using Microsoft Visual Basic (Version 6.0).

The user interface displays the setting temperature, the sensing temperature, swing ON/ OFF and the fan speed of the air conditional system as shown in Fig.5. In this system, the temperature sensors are used to sense the condition of room.

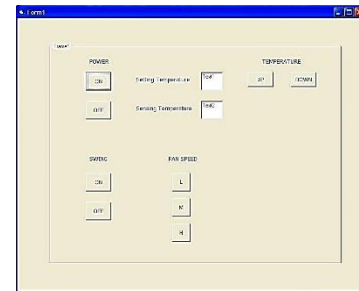


Fig. 5 Graphical User Interface for Air Con Control System

3.3 Software Development for the System

For software development for SCADA based air-conditioning system, the assembly language for AT89S51 microcontroller is used to develop a control process for temperature sensing system, stepper motor, variable speed fan motor and compressor. The main control process is shown in Fig. 6.

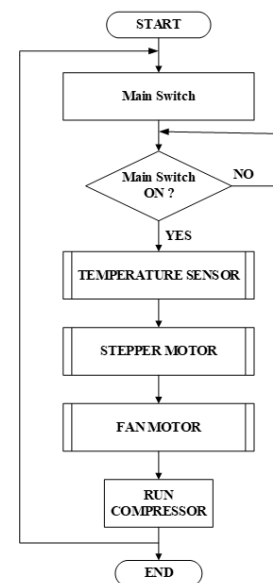


Fig. 6 Main Flowchart of the System

3.4 Software Development for Temperature Sensing

The temperature sensed by the room temperature sensor is greater than or equal to setting temperature by GUI from PC, the compressor and cooling fan in outdoor unit of the air-conditioning system will be run automatically, otherwise it will be shutdown.

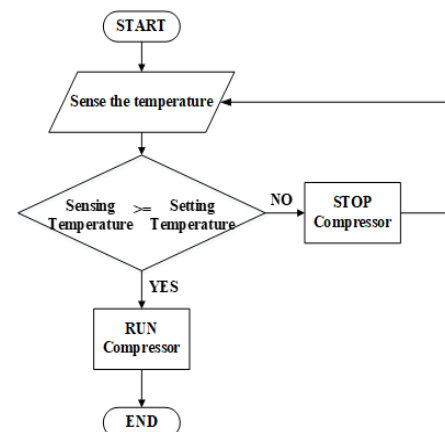


Fig. 7 Flowchart of Temperature Sensing

3.5 Software Development for Indoor Fan Control

The indoor fan can be switched ON and OFF and its speed can be changed by three kinds of switches—low, medium and high in GUI from PC. If one of three switches is in ON condition, the other two switches will be OFF.

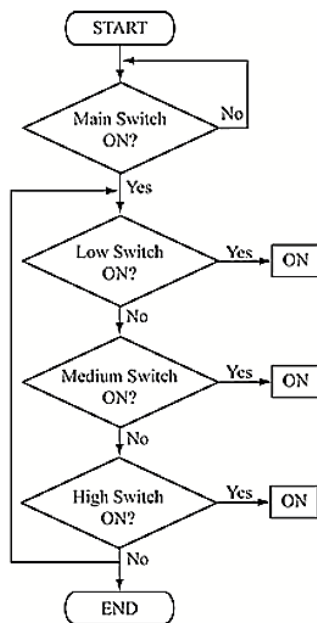


Fig. 8 Flowchart of Indoor Fan Control

3.6 Software Development for Stepper Motor Control

The stepper motor control process for swing function includes main ON/OFF and automatic forward and reverse running mode. If the main switch is ON condition, the stepper motor will run in forward direction until sensor 2 is High state. The stepper motor will run in reverse direction once the sensor 1 is High state. The flow chart of the stepper motor for swing function is shown in Fig. 9.

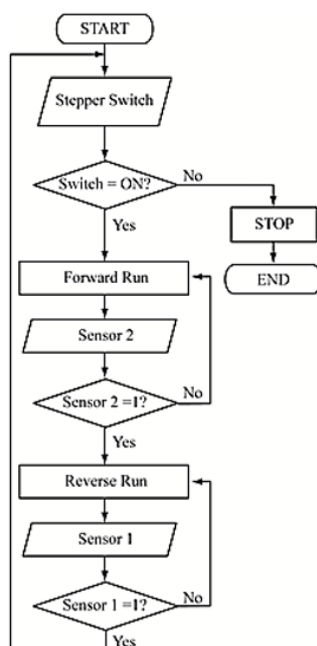


Fig. 9 Flowchart of Stepper Motor Control

4. TESTS AND RESULTS

Software simulation test has been run before hardware test and implementation. The main engineering software tool used in this research work for simulation is Proteus 7 professional. Each portion of SCADA Air-conditioning system is developed and tested in Proteus simulator. Some critical simulations, tests and results of the system are described as follows.

4.1 Simulation Test for Stepper Motor Control

The simulation circuit for stepper motor control by AT89S51 microcontroller is shown in Fig. 10. If the input switch is HIGH state, the microcontroller will produce a PWM and stepper motor will run and otherwise it will stop.

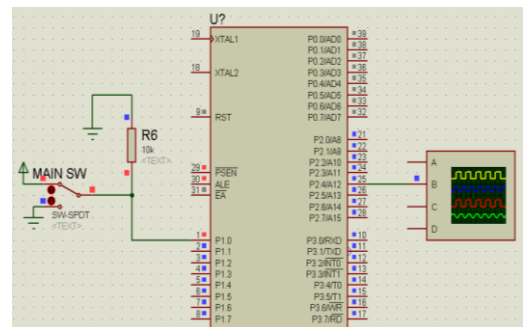


Fig. 10 Simulation Test for Stepper Motor Control Circuit

The main function of microcontroller for stepper motor control is to produce PWM that is suitable for stepper motor speed. The 8051 microcontroller provides a PWM which is frequency 5 Hz and 50 % duty cycle. The waveform of PWM is shown in Fig. 11. According to testing results, this PWM can run the stepper motor in suitable speed for swing function of indoor unit fan.

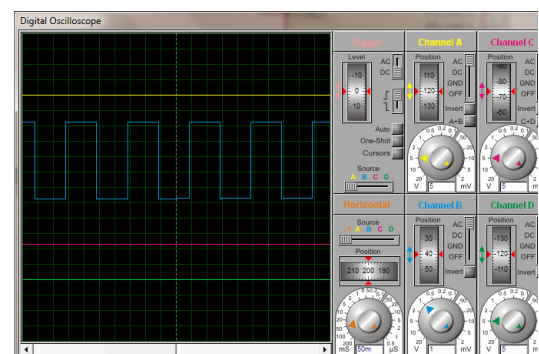


Fig. 11 PWM Waveform of Stepper Motor Driven Signal

For driving the stepper motor in forward and reverse rotation, the pin 26 of port 2 produces the control signal, low and high, in turn automatically. When this pin is in high state, the stepper motor will rotate in forward rotation for 15 seconds. And then, the pin 26 will be again in low state in result of reverse rotation of stepper motor. The simulation test of stepper motor rotation is shown in Fig. 12.

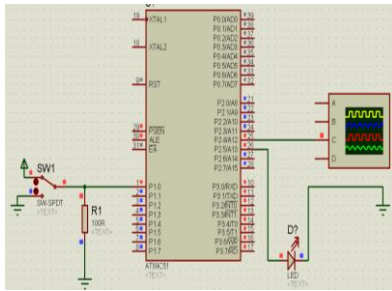


Fig. 12 Simulation for Forward and Reverse Rotation of Stepper Motor

4.2 Simulation Test for Temperature Sensing Unit

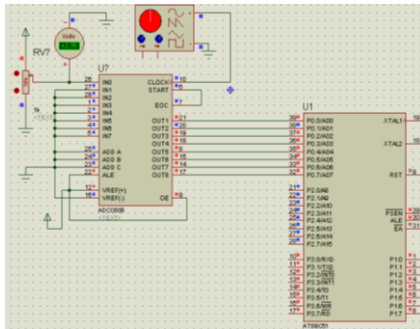


Fig. 13 Simulation of Temperature Sensing Unit

Instead of temperature sensor, the potentiometer is used to provide changing analog voltages into 8 bits ADC. The clock for ADC 0808 is provided by function generator. The simulation test of ADC 0808 and AT89S51 microcontroller interfacing is shown in Fig. 13. According to the simulation, it can be seen that the different analog values equivalent to the different temperature values can be converted to correct digital values by ADC0809 and its output is forwarded to microcontroller input for comparing with setting temperature value.

4.3 Hardware Test

The MAX232N IC is used for interfacing the main control circuit and personal computer. The interfacing test for main controller and PC is shown in Fig. 14. The status of the communication between PC and main control circuit is checked by reading the status of GUI on the PC and LED on the main control circuit. According to the result of the test, PC and main controller can communicate well with each other through MAX232.

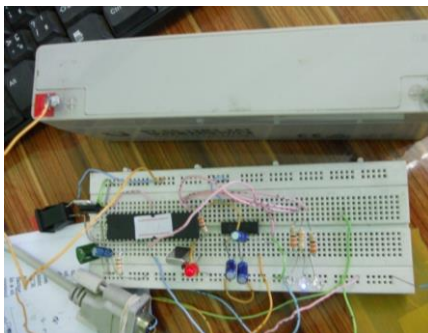


Fig. 14 Interfacing Test for PC and Main Controller

The control circuit of DC motor and stepper motor is tested as mentioned in Fig. 15. Forward and reverse condition of DC and stepper motors are tested with respective driver circuits. According to the test, it can be seen that DC motor and stepper motor can run and respond well to the commands of the main control circuit, and the driver circuits can also handle their respective control devices.

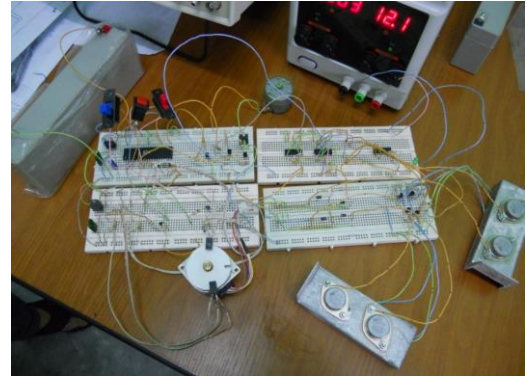


Fig. 15 Testing of Control Circuit for Stepper Motor and DC Motor

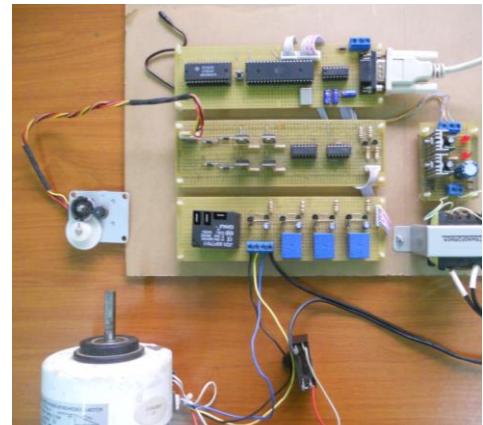


Fig. 16 Testing of Final Assembly Circuit

After step-by-step test for each hardware portion has been done, the final assembly circuit has been tested as shown in Fig. 16. Not only the hardware but also the communication between PC and this control circuit is tested. After fine tuning and calibration, the response of the overall system is tested in real environment. The response of the system for different temperature settings and strategies is checked. The findings for these tests are discussed in the following section.

4.4 Results

The temperature distribution for human comfort is achieved through the control of air conditioner flaps or vane control. The resulting temperature distribution for the whole room is almost uniform because of using several sensors throughout the room and the air blowing direction is changing according to the user setting.

According to tests on the system, two significant findings regarding the use of multiple sensors for controlling systems with three actuators have been noted. The first one is that using multiple sensors can

result in simultaneous energy savings and comfort improvement. The second one is that all strategies for using multiple sensors work better than a single sensor strategy.

5. CONCLUSIONS

Supervisory Control and Data Acquisition (SCADA) system is a sophisticated automation, data acquisition and data logging tool as well as a control option during operation, thus facilitating operators to effect parameter changes based on actual real time data available at his fingertips. The facility to view key process parameters like, temperature, operation of compressor, swing, fan speed, allows the operating personnel to analyze and instantaneously take corrective action. The optimized utilization of equipment running time manifests as reduced energy consumption. The real time consumption trend helps in overall optimization, leading to energy savings.

The exploit of modern materials and equipment with the implementation of appropriate algorithms produce modern air-conditioning systems that belong to the energy saving with maximum performance. A system for monitoring and control provides management and visualization of the object and display the current value of significant parameters. With the stored data in the system, it is possible to detect the problems with the On/Off controllers applied to the air conditioning system. The program embedded in the microcontroller can be changed as the user's requirement without needing to change the design of air conditioning parts.

ACKNOWLEDGEMENT

The authors would like to thank all persons who involved towards the successful completion for this research work.

REFERENCES

- [1] T.H Kim, "Integration of Wireless SCADA through the Internet," International Journal of Computers and Communications, Issue 4, Volume 4, 2010.
- [2] slideshare.net [Online]. Available: <https://www.slideshare.net/TheRealAkansha/scada-ppt>
- [3] Difference between DCS and SCADA by Rushi Shroff [Online]. Available: <https://control.com/forums/threads/difference-between-dcs-and-scada.40986/>
- [4] EPCOS Application note, 2013 [Online]. Available: <https://www.tdk-electronics.tdk.com/download/539016/42896f24ac533f49f0fac5b0ff8a40b0/pdf-sensorsairconditioningautomotive-an1.pdf>
- [5] ADC0809-n datasheet [Online]. Available: <http://www.ti.com/lit/ds/symlink/adc0808-n.pdf>
- [6] AT89S51 datasheet [Online]. Available: <http://ww1.microchip.com/downloads/en/devicedoc/doc2487.pdf>

REAL TIME DRIVER FATIGUE AND YAWN DETECTION BASED ON FACIAL LANDMARKS ANALYSIS USING OPENCV AND DLIB LIBRARY

Theint Theint Ei⁽¹⁾, Moe Mon Myint⁽²⁾, Khin Thuzar Linn⁽³⁾

⁽¹⁾ Pyay Technological University, Myanmar

⁽²⁾ Pyay Technological University, Myanmar

⁽³⁾ Pyay Technological University, Myanmar

Email: ladie.mmo@gmail.com

ABSTRACT: Traffic accidents due to human errors cause many deaths and injuries around the world. The raising number of traffic accidents is principally caused by fatigue. Safe driving is a major concern of communities all over the world. Eye and mouth state analysis is an important step in fatigue and yawn detection. The system involves image acquisition from webcam, Dlib facial 68 landmarks detector for face, eyes, mouth, fatigue with eye aspect ratio (EAR) and yawn detection. The system using OpenCV library is based on the real time facial images analysis. This system processes live video feed concentrated on the driver's face and tracks the user eye and mouth movements to detect eye closure and yawning rates. Main coding language is python language. Blinks, fatigue levels and yawning rates are displayed on monitor screen with fatigue and yawn detection using alert message. In this system, the threshold EAR value is 0.2 and yawning rate is 20. The average range of EAR values of this system are 0.3076 (eyes open), 0.1827 (eyes blink) and 0.1534 (eyes close). Average range of yawn values is 20. Average yawn values of this system are 22.8571 (opening mouth), 9.7143 (small opening mouth or talking) and 5.857 (closing mouth).

KEYWORDS: *eye aspect ratio (EAR), python, Dlib, OpenCV, yawn detection, fatigue detection*

1. INTRODUCTION

The fatigue of the driver can lead to road accidents. With the growth of computer vision and image processing technology, it is now feasible to investigate this problem [1]. In recent years, driver fatigue has become one of the most main factors for traffic accidents, which has come at a great cost to the safety and property of drivers and walkers [2]. These accidents can be controlled by growth of technologies for detecting or preventing fatigue.

Many fatigue detection methods can be classified into three types: physiological parameters, vehicle behaviors, and facial feature analysis. There are many signs of the driver's fatigue. Driver may be yawn frequently, is unable to keep eyes open, catches him nodding off and has trouble keeping head up and can't remember driving the last few miles [3]. This system is a non-complex method which did not require any training of the data.

This system work is focused on the localization of the eyes and mouth of the face image, and determining the situation of the eyes and mouth, by a proposing well image processing algorithm. This system proposes a computer vision based driver fatigue and yawn system, use of OpenCV in real-time image or video processing, interfacing of web camera, Dlib facial landmark detector constructed face detection methods. In this non-intrusive method, the main techniques used for eye blink detection is Eye Aspect Ratio (EAR) method and yawning rate is yawn detector in Dlib library. The former state is characterized by a moment of close eyes and the latter is identified by a prolonged state of open mouth or yawning. This system is essential to develop a real time safety system for fatigue related road accident prevention.

2. BACKGROUND THEOREY

Fatigue detection can be divided into three main aspects such as vehicle based method, behavioral based method and physiological based method [4]. Fatigue detection is established on the above mentioned categories.

2.1 Vehicle Based Fatigue Detection System

This type is based on different mechanical parts of the vehicle such as steering wheel movement, deviation from the lane position, speed of the vehicle etc [5]. All these mechanical parts are detected continuously and if these parts cross a specified threshold value then it is predicted that the driver is in fatigue state.

2.2 Behavioral Based Fatigue Detection System

This category is based on different behaviors of head such as head pose changing, eye closure or blinking, yawning, etc. All these behaviors are constantly detected and monitored through a camera. The driver is alerted if any of these signs are detected.

2.3 Physiological Based Fatigue Detection System

This type is based on physiological signals like ECG (Electrocardiogram) and EOG (Electrooculogram). Driver fatigue detection can be done through pulse rate, heart beat and brain information [6].

3. METHODOLOGY

Process flow of the proposed algorithm is shown in Fig 1, which steps takes place for fatigue and yawn detection. The video feed used in testing this system is obtained from laptop webcam.

3.1 Pre-processing

The video is obtained from a webcam focused on the driver's face. The processing rate of the acquired video is 30 frames per second. These frames are flipped and converted to grayscale.

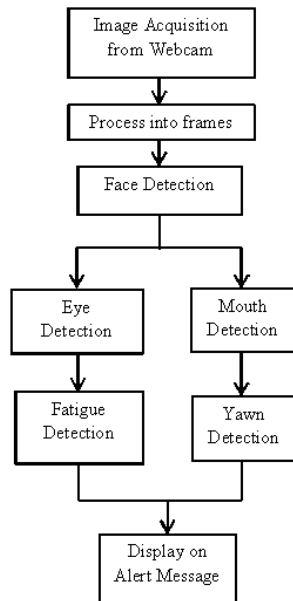


Fig 1. Process Flow of the System

3.2 Dlib Face Detection

This system uses Dlib and OpenCV to detect face and facial landmarks detection in an image. Dlib for facial landmark detection is applied to find and locate the face in the image. It initializes Dlib pre-trained face detector based on a modification to the standard histogram of oriented gradients (HOG) and linear SVM. The frontal face detector in Dlib operates really well [7].

Facial landmarks are manipulated to localize and represent salient regions of the face such as eyes, eyebrows, nose, mouth and jawline. Facial landmarks have been successfully affected to face alignment, head pose estimation, face swapping, blink detection and much more. The shape_to_np and NumPy array function are utilized to detect facial landmarks in images.

3.3 Facial Mapping using Dlib

The algorithm is applied using Dlib python library that contains a landmark's facial detector with pre-trained models. It evaluates and maps a person's face in the form of facial points with 68 cartesian co-ordinates as shown in Fig 2. The 68-point iBUG 300 dataset was used to train the Dlib facial landmarks predictor and is the source of these markings.

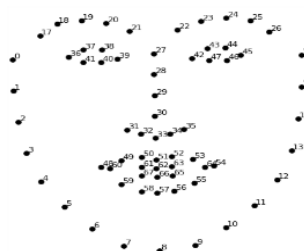


Fig 2. Facial Landmark Points

3.4 Eye Closure Detection

Eye aspect ratio (EAR) is a parameter that decides eye state used to figure out if it is opened or closed. It can be computed using facial landmarks plotted by the 68 facial landmark point plot provided by python's Dlib library. It uses the points in the region of interest to calculate eye closure. The eye aspect ratio can be defined by the equation (1) [8].

$$EAR = \frac{\|P_2 - P_6\| + \|P_3 - P_5\|}{2\|P_1 - P_4\|} \quad (1)$$

Equation (1) is used to compute EAR value and $P_1, P_2, P_3, P_4, P_5, P_6$ are the boundary landmarks from the region marked to contain the eyes as shown in Fig 3. In Fig 3, P_2, P_3, P_5, P_6 are the vertical landmarks on the eye and P_1, P_4 are the horizontal eye landmarks. A blink is detected when the calculated value is below 0.2. The threshold value set in this algorithm is 0.2. If this continues consecutively for 5 frames, eye blink is confirmed. This state is driver fatigue condition.

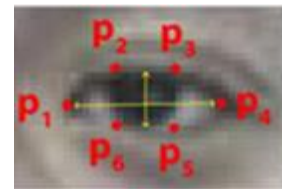


Fig 3. Open Eye with Landmarks

3.5 Yawn Detection

Yawn detector using Dlib library which is all about detecting yawn which involuntarily open one's mouth wide and inhale deeply due to tiredness or boredom. This system deals with using yawn detector in Dlib library for extracting facial landmark from live webcam feed of the driver, and using OpenCV to detect distance between the lips and classify it as a yawn and inform as an alert message when the driver is yawning. A widely opened mouth represents yawning state [9]. The facial landmarks are used to detect an open mouth. Mean value of lip distance or yawning rate is calculated from top lip center subtract bottom lip center. If mean value of lip distance is greater than lip distance threshold, the driver is determined to be yawning. Small openings such as talking and eating are ignored.

The region marked to contain the mouth as shown in Fig 4. Mean value of top lip center point is computed from the facial landmarks of mouth point of 50 to 53 and 61 to 64. Mean value of bottom lip center point is computed from the facial mouth landmarks point of 56 to 59 and 65 to 67. Then, lip distance is computed subtracting from mean value of top lip center point to mean value of bottom lip center point. Fig 5 shows flow chart of the algorithm.

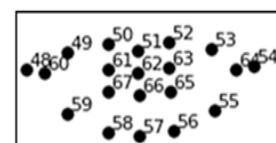


Fig 4. Facial Mouth Landmarks

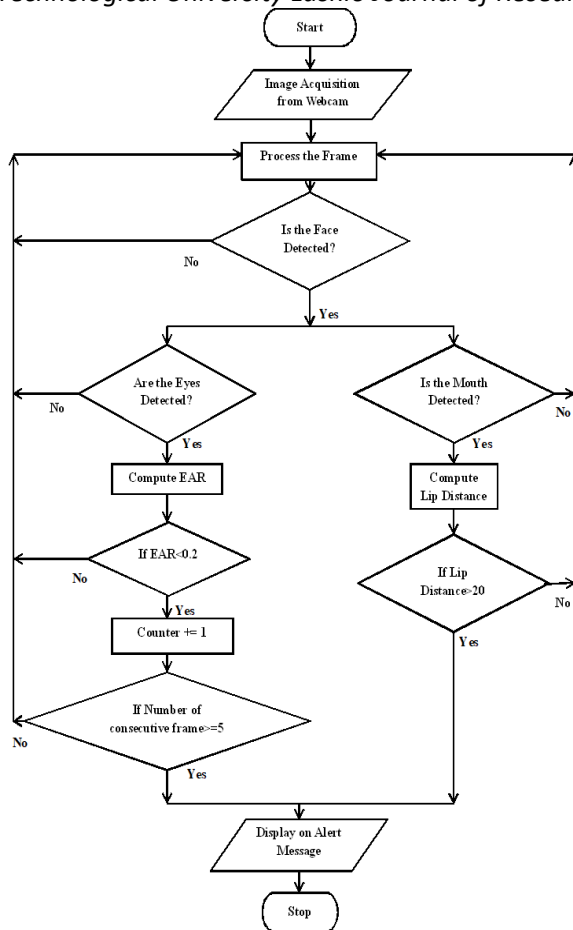


Fig 5. Flow chart of the algorithm

4. IMPLEMENTATION

The implementation of fatigue and yawn detection system can be primarily performed by two methods which the number of eye blinking and the yawning rate. Based on these two parameters, a driver can be identified whether driver is drowsy or not. Whenever the user is drowsy, the eye closure value decreases the EAR threshold value and the yawn value increases the yawn threshold value then an alert message must be displayed on the screen.

Initially, the required libraries for the python code are loaded which help in various functionalities while executing the algorithm. The computer vision-based system checks for fatigue and yawn detection of the driver by tracking the user's face in real-time. An alert message is displayed on the screen if the user is found drowsy. A facial landmarks file is imported into this algorithm which is utilized to trace the coordinates of the facial features for an individual. These coordinates are helpful while drawing the contours around the features and keeping track of the eyes and mouth distance ratio. The pattern and edge detection are performed using the functions from Imutils library.

The entire frame of the image is converted into a grayscale image. The OpenCV library supports in detecting the real time image of driver's face from the frame.

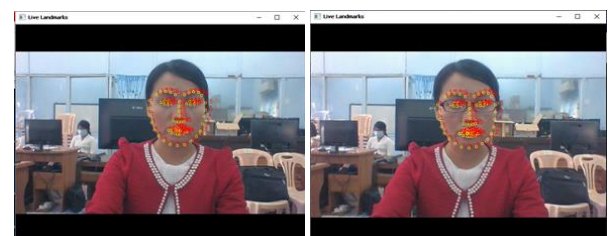
To determine the eye closure is taken so as to calculate the eye aspect ratios (EAR), which the ratio of

distances between the vertical eye landmarks and the distances between the horizontal eye landmarks. A specific Euclidean function can be applied here to compute the distance between two eyes. Similarly, the mouth distance is also calculated for estimating the yawning rate.

Whenever the person gets drowsy, the distance between both the eyelids is reduced and the distance between both the lips distance increases when the person yawns. For five consecutive frames, if the eye aspect ratio value is found to be less than 0.2, an alert message, "Driver Fatigue Detected", will be displayed on the screen. If mean value of lip distance is greater than threshold value of lip distance, an alert message, "Driver is Yawning", will be also displayed on the screen.

5. EXPERIMENTAL RESULTS

Fig 6(a) shows the person's face detection with facial landmarks points without spectacles and Fig 6(b) shows the person's face detection with facial landmarks points with spectacles.

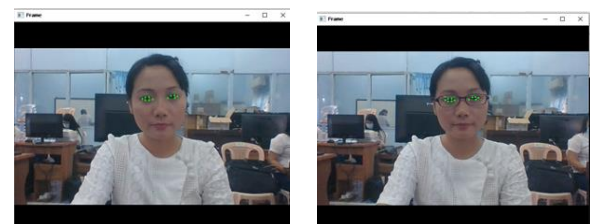


(a)

(b)

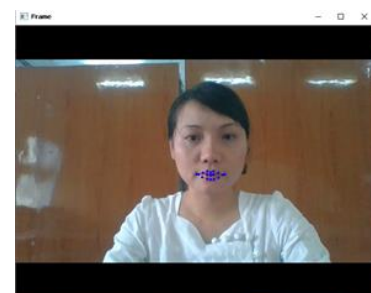
Fig 6.(a) Face detection without spectacles (b) Face detection with spectacles

Fig 7(a) shows the person's eyes detection without spectacles, Fig 7(b) shows the person's eyes detection with spectacles and Fig 7(c) shows the person's mouth detection.



(a)

(b)



(c)

Fig 7. (a) Eye detection without spectacles (b) Eye detection with spectacles (c) Mouth detection

Fig 8(a) shows EAR values of 0.3099 when the person's eyes opened without spectacles. Fig 8(b) shows EAR value of 0.1899 when the person's eyes blinked without spectacles. When the person's eyes closed without spectacles, EAR value of 0.163 and fatigue detection with alert message are shown in Fig 8(c).

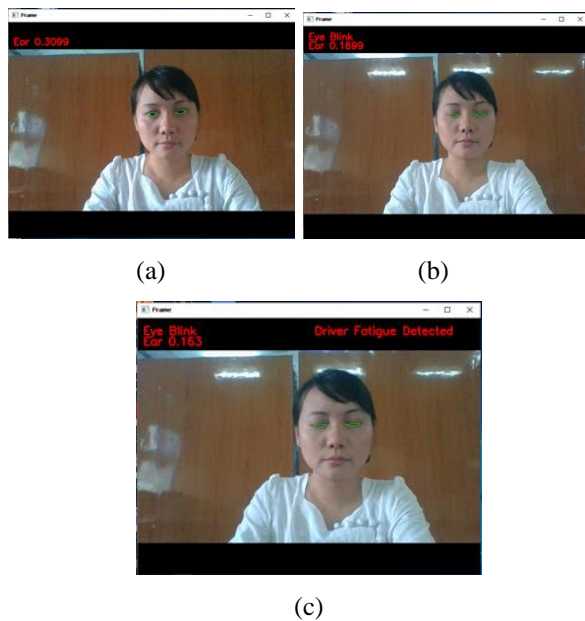


Fig 8. (a) EAR value when the person's eyes opened without spectacles (b) EAR value when the person's eyes blinked without spectacles (c) EAR value when the person's eyes closed without spectacles

EAR value of 0.2738 when the person's eyes opened with spectacles is shown in Fig 9(a). EAR value of 0.1807 when the person's eyes blinked with spectacles is shown in Fig 9(b). Fig 9(c) shows EAR value of 0.1388 when the person's eyes closed with spectacles and fatigue detection with alert message.

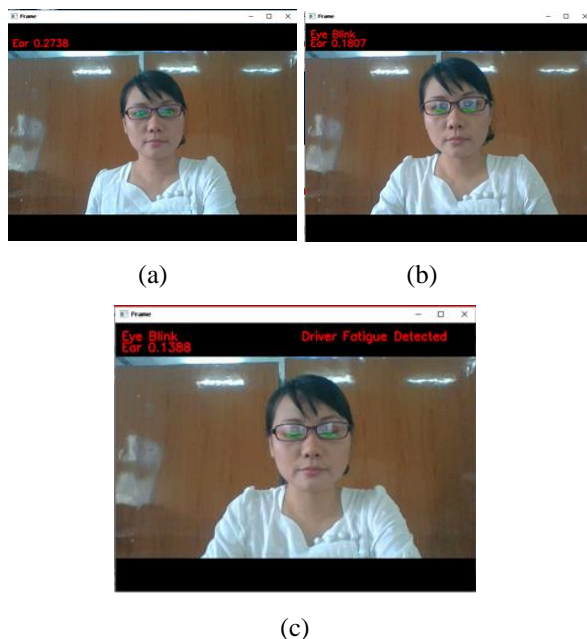


Fig 9. (a) EAR value when the person's eyes opened with spectacles (b) EAR value when the person's eyes blinked

with spectacles (c) EAR value when the person's eyes closed with spectacles

Table 1. AVERAGE VALUE OF EAR FROM SEVEN PERSONS

Person	EAR for open eyes	EAR for blink eyes	EAR for close eyes
1	0.3099	0.1899	0.1630
2	0.2969	0.1999	0.1459
3	0.3271	0.1774	0.1348
4	0.2738	0.1807	0.1388
5	0.2869	0.1829	0.1741
6	0.3849	0.1673	0.1782
7	0.2738	0.1807	0.1388
Average	0.3076	0.1827	0.1534

The calculated average value of EAR obtained from the seven persons as shown in Table 1. The average eye aspect ratio is 0.3076 when the eyes opened, 0.1827 when the eyes blinked and 0.1534 when the eye closed, respectively.

Fig 10(a) shows yawn value of 6 when the person's mouth is closing. Fig 10(b) shows yawn value of 12 when the person's mouth is small openings such as talking. Fig 10(c) shows yawn value of 22 when the person's mouth is opening and yawn detection with alert message

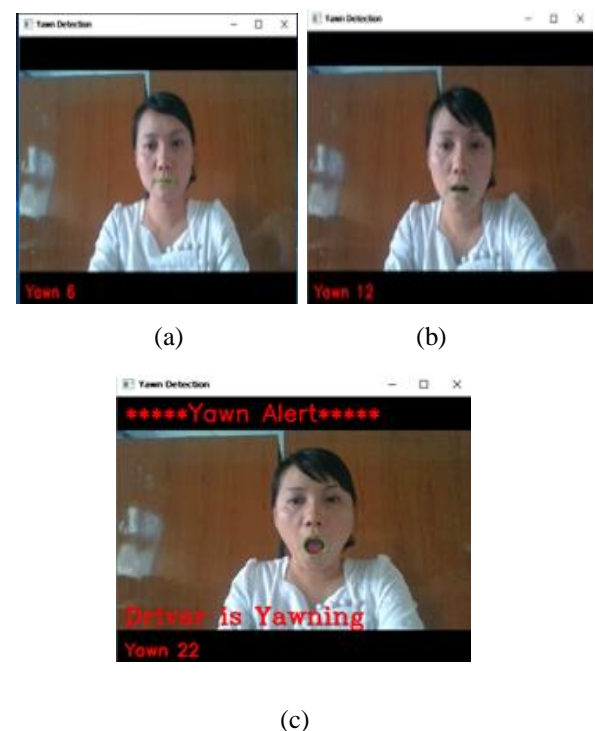


Fig 10. (a) Yawn value when the person's mouth is closing (b) Yawn value when the person's mouth is small openings such as talking (c) Yawn value when the person's mouth is opening

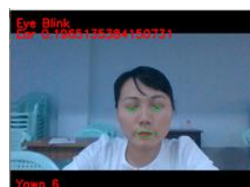
Table 2. AVERAGE VALUE OF YAWNING FROM SEVEN PERSONS

Person	Yawning rate for open mouth state	Yawning rate for talking mouth state	Yawning rate for close mouth state
1	21	9	4
2	22	8	5
3	22	7	6
4	22	12	6
5	27	10	6
6	22	8	7
7	24	14	7
Average	22.8571	9.7143	5.8571

Table 2 shows the calculated average value of yawning rate obtained from the seven persons of different condition. The average yawn value for opening mouth is 22.8571, the average yawn value for small opening mouth is 9.7143 and the average yawn value for closing mouth is 5.857, respectively. From the tests and results, yawn value for open mouth is greater than threshold yawn value and yawn values for small opening mouth and close mouth are less than threshold yawn value. So, yawn threshold value of 20 is suitable for this system. Yawn value of 6 and EAR value of 0.3279 when the person's eyes opened without spectacles is shown in Fig 11(a). Fig 11(b) shows yawn value of 6 and EAR value of 0.1965 when the person's eyes blinked without spectacles. Fig 11(c) shows yawn value of 7 and EAR value of 0.1477 when the person's eyes closed without spectacles and fatigue detection with alert message.



(a)



(b)



(c)

Fig 11. (a) Yawn and EAR value when person's eyes opened without spectacles (b) Yawn and EAR value when person's eyes blinked without spectacles (c) Yawn and EAR value when person's eyes closed without spectacles

Fig 12(a) shows yawn value of 7 and EAR value of 0.2865 when the person's eyes opened with spectacles. Fig 12(b) shows yawn value of 7 and EAR value of 0.1682 when the person's eyes blinked with spectacles. Fig 12(c) shows yawn value of 6 and EAR value of 0.1606 when the person's eyes closed with spectacles and fatigue detection with alert message.



(a)



(b)



(c)

Fig 12. (a) Yawn and EAR value when the person's eyes opened with spectacles (b) Yawn and EAR value when the person's eyes blinked with spectacles (c) Yawn and EAR value when the person's eyes closed with spectacles

Fig 13(a) shows EAR value of 0.2798 and yawn value of 10 when the person's mouth is closing. Fig 13(b) shows EAR value of 0.1853 when the person's eyes blinked with spectacles and yawn value of 14 when the person's mouth is small openings such as talking. Fig 13(c) shows EAR value of 0.3236 and yawn value of 24. In this state, the person's mouth is opening and the yawn detection with alert message is displayed.



(a)

(b)



(c)

Fig 13. (a) EAR and Yawn value when the person's mouth is closing (b) EAR value and Yawn value when the person's eyes blinked with spectacles and the person's mouth is small openings (c) EAR and Yawn value when the person's mouth is opening

Fig 14(a) shows EAR value of 0.1799 when the person's eyes closed without spectacles and displays fatigue detection with alert message. In this state, yawn values of 25 when the person's mouth is opening and yawn detection with alert message are displayed. Fig 14(b) shows EAR value of 0.1597 when the person's eyes closed with spectacles and displays fatigue detection with alert message. In this condition, yawn values of 22 when the person's mouth is opening and yawn detection with alert message are displayed, respectively.



(a)



(b)

Fig 14. (a) Fatigue and yawn detection with alert message without wearing spectacles (b) Fatigue and yawn detection with alert message wearing spectacles

Table 3. ACCURACY OF FATIGUE AND YAWN DETECTION FOR TEN PERSONS

Type of Detection	Fatigue Detection	Yawn Detection	Both Fatigue and Yawn Detection
TP	10	9	8
TN	10	10	10
FP	0	0	0
FN	0	1	2
Accuracy	100%	95%	90%

The detection accuracy can be defined by the equation (2).

$$Accuracy = \frac{TP + TN}{(TP + TN + FP + FN)} \times 100 \quad (2)$$

In the experiment, the fatigue and yawn activities could be identified by fatigue detection, yawn detection, or both if performed simultaneously by the person. In equation (2), true positive (TP) condition is applicable when the model detected true fatigue or yawn activity, true negative (TN) is when non-fatigue or non-yawn activity is correctly distinguished by the model, false positive (FP) is when the system detects fatigue or yawn activity that is supposedly none, and false negative (FN) for fatigue or yawn activity that is incorrectly detected.

Ten peoples are tested the model consisting of seven males and three females with wearing eye-glasses and without wearing eye-glasses. Each person was requested to perform eye blinking, yawning, and both. Table 3 shows the result of the detection accuracy of fatigue and yawn. The developed model could easily detect the eye blink, reaching a 100% accuracy in performance and yawning detection is 95%. However, the combined eye-based and mouth-based fatigue activities achieved a low accuracy rate with 90% - mainly because there were instances that both eye blinking and yawning were not performed simultaneously which then resulted to some false detection. The overall performance accuracy is 90%.

6. CONCLUSION AND FUTURE WORK

The system detects fatigue in a driver using eye blinking and yawning as indicators. The system is tested on a variety of persons and conditions. The system used OpenCV, python, and Dlib open source Libraries by measuring EAR and yawning rate.

The eye aspect ratio for each eye can be computed using Euclidian distance functions of OpenCV. The yawning rate can be calculated from the top lip center subtract the bottom lip center.

The eye aspect ratio is calculated, if a person is blinking, the eye aspect ratio is less than threshold value. The duration of blink further provide estimation of fatigue. The system works for people wearing spectacles. Yawning rate is calculated, if a person is yawn, the mean value of lips distance is greater than threshold yawn value, then decrease again as the mouth close. This system is tested in various persons and different conditions.

The system is tested accuracy of fatigue and yawn detection for various ten persons. The accuracy of fatigue detection is 100%, accuracy of yawn detection is 95% and accuracy of both fatigue and yawn detection is 90%. The accuracy of system performance is 90%.

These systems can be used in various major applications like self-driving cars, driver's fatigue detection, driver's drowsiness detection, driver's consciousness detection etc. The system can be used in vehicles, locomotives, flights and waterways. The system protects human resources and damage things. In the future work, this algorithm can be used as a base and can be implemented in an Android application through API calls. This application can be implemented in real-time to avoid accidents caused by driver's fatigue.

ACKNOWLEDGEMENT

Firstly, the author would like to acknowledge particular thanks to Dr. Nyunt Soe, Rector of the Pyay Technological University. The author would like to express her thanks to Dr. Mya Thandar Kyu, Professor and Head of the Department of Electronic Engineering, Pyay Technological University, for her helpful guidance of this paper. The author is greatly indebted to her supervisor Dr. Moe Mon Myint, Professor, Department of Electronic Engineering, Pyay Technological University, for her enthusiasm, patience, continuous supervision, effective suggestions, and skillful guidance throughout this paper. The author would like to express her thanks to her co-supervisor Daw Khin Thuzar Linn, Associate Professor, Department of Electronic Engineering, Pyay Technological University, for her patience and invaluable assistance throughout the paper.

REFERENCES

- [1] Anna Liza A. Ramos, Jomar Christian Erandio, Dean Hur T. Mangilaya, Nathaniel Del Carmen, Erika May Enteria and Leonilo Jean Enriquez, "Driver Drowsiness Detection Based on Eye Movement and Yawning Using Facial Landmark Analysis," DOI 10.5013/IJSSST.a.20.S2.37, ISSN: 1473-804x, 2018
- [2] Yingyu Ji, Shigang Wang, Yang Lu, Jian Wei and Yan Zhao, "Eye and mouth state detection algorithm based on contour feature extraction," J. Electron. Imaging 27(5), doi: 10.1117 /1. JEI.27 .5.051205, 051205, 2018.

- [3] A. Deepa Lakshmi, B. Nivetha, A. Jaya Kumar and R. Malar, "The Literature Survey Based On Car Safety System," e-ISSN: 2278-067X, p-ISSN: 2278-800X, www.ijerd.com, Volume 11, Issue 11, PP.42-44, November 2015.
- [4] Jyotsna Gabhane, Dhanashri Dixit, Pranali Mankar, Ruchika Kamble and Sayantani Gupta, "Drowsiness Detection and Alert System: A Review," IJRASET, Vol 06 Issue:04, April 2018
- [5] Pankti P. Bhatt and Dr. Jeegar A. Trivedi, "Various Methods for Driver Drowsiness Detection : An Overview," IJCSE, ISSN : 0975-3397, Vol. 9 No.03 Mar 2017
- [6] Arun Sahayadhas, Kenneth Sundaraj and Murugappan Murugappan "Detecting Driver Drowsiness Based on Sensors: A Review," ISSN 1424-8220, 16937-16953; doi:10.3390/s121216937, 7 December 2012
- [7] Miss. Ankita M. Bhoyar and Prof. S. N. Sawalkar, "Implementation on Visual Analysis of Eye State Using Image Processing for Driver Fatigue Detection," IRJET, e-ISSN: 2395-0056, p-ISSN: 2395-0072, vol. 06 Issue: 04, Apr 2019.
- [8] Akalya Chellappa, Mandi Sushmanth Reddy, R. Ezhilarasie, S. Kanimozhi Suguna and A. Umamakeswari, "Fatigue Detection Using Raspberry Pi 3," IJET, DOI: 10.14419/ijet, vol. 07, I 2.24.11993, April 2018
- [9] Zhuoni Jie, Marwa Mahmoud, Quentin Stafford-Fraser, Peter Robinson, Eduardo Dias and Lee Skrypchuk, "978-1-5386-2335-0/18, IEEE, 2018

Microcontroller based Home Automation System

Thinn Thinn Htwe⁽¹⁾, Thida Aung⁽²⁾, Shwe Yee Win⁽³⁾

⁽¹⁾Technological University (Meiktila), Myanmar

⁽²⁾ Technological University (Lashio), Myanmar

⁽³⁾ Technological University (Lashio), Myanmar

Email: thinthinhtwe@tumeiktila.edu.mm

thidaaung@tulashio.edu.mm

shweyeewin@tulashio.edu.mm

ABSTRACT: This paper presents the microcontroller based home automation system. It uses a grouping of hardware and software technologies that enable control and management over appliances and devices within a home. This system uses sensors to make automatically the home appliances. These sensors are motion sensor, gas sensor, temperature sensor and light dependent resistor (LDR). The implementation and design of wireless home automation control has used two modules: Global System for Mobile Communication (GSM) module for controlling home appliances from anywhere and Bluetooth module at home. This system have been used Arduino Software for programming.

KEYWORDS: *Arduino Mega, GSM module, bluetooth module, motion sensor, temperature sensor, gas sensor*

1. INTRODUCTION

Smart home automation systems take part in an essential role in making daily life more comfortable and facilitate users from ceiling fan to other applications. In this regard, control of lighting system using LDR, Passive Infrared sensor (PIR) and Arduino. Some of the major communication technologies are used by home automation system include Bluetooth, Wireless LAN (Wi-Fi) and GSM. GSM is one of the most broadly used cellular technologies in the world. The home automation system is based on Short Message Service (SMS) technology using Arduino Mega 260 microcontroller. The microcontroller acts as the bridge between the GSM modules and sensors of the home automation system. [1][3]

The sensors are MQ135 gas sensor, LM35 temperature sensor and PIR motion sensor. When gases and air pollution appear in the home, the gas sensor will be active. The temperature sensors can be made automatically on/off the fan. The user can send commands via SMS. GSM module transfers it to the Arduino Mega 2560 microcontroller. The microcontroller then operates the devices according to the command received. The project can be used as remote device control. It will help to control and operate devices while the users are not able to access them physically.

Smart home automation system is also used Bluetooth HC-06 module when the user reaches the home. The user can control the home appliance with Bluetooth module using Android based smart phone application. The

Bluetooth module is connected with the Arduino. The Arduino receives the data from the Bluetooth module and command to electrical components which items should be ON or OFF. [2]

Figure 1 shows the block diagram of the home automation system.

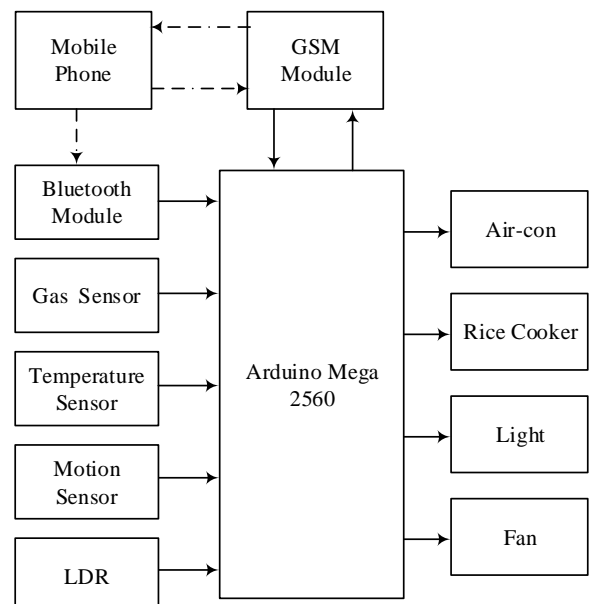


Fig 1. Block Diagram of Microcontroller based Home Automation System

2. THEORETICAL BACKGROUND

Today's smart homes are more about safety and living greener. Smart home automation consist of remote mobile controls, automated lights, automated thermostat Adjustment, scheduling appliances, mobile, email, text notifications and remote video surveillance.

There are many specifications of home automation system based on various methodologies.

2.1 Bluetooth Based Home Automation System

In Bluetooth based home automation system, the home appliances are connected to the Arduino BT board at input and output ports using relay. The program of Arduino BT board is based on high level interactive C language of microcontrollers; the connection is made via Bluetooth. The Arduino BT board has a range of 10 to 100meters, 3Mbps data rate and 2.4GHz bandwidth. The password protection is provided so only authorized user is allowed to access the appliances. The Bluetooth connection is

recognized between Arduino BT board and phone for wireless communication. It has the advantage to easily fit into an existing home and automated system. The main disadvantage of system is that it is limited to control the home appliances within the Bluetooth range. [2]

2.2 GSM Based Home Automation System

The proposed system is GSM based home automation system. The proposed home automation system allow user to switch ON and OFF the lights, fans etc. from everywhere since this system is restricted using GSM module. The idea behind this is to get the send message string from cell phone and then processing it to carry out the desired function. [6]

3. Required System Components

The required system components are Arduino Mega, GSM module, Bluetooth module, MQ-135 gas sensor module, LM35 temperature sensor, PIR motion sensor and LDR.

3.1 Arduino Mega

A microcontroller **Arduino Mega 2560** board is based on the **ATmega2560**. It is built of 54 digital input/output pins (of which 15 can be used as PWM outputs), 16 analog inputs, 4 UARTs (hardware serial ports), a 16 MHz crystal oscillator, a USB connection, a power jack, an ICSP header, and a reset button. It is simply connected to a computer with a USB cable or power with a AC-to-DC adapter or battery to get started.



Fig 2.Arduino Mega 2560 [7]

3.2 GSM Module

GSM Modules are one of the commonly used communication modules in embedded systems. A GSM/GPRS Module is used to enable communication between a microcontroller and the GSM Network. GSM modules allow microcontrollers to have a wireless communication with other devices and instruments.



(a)



(b)

Fig 3.(a) GSM Module [3] (b) Bluetooth Module [5]

3.3 Bluetooth Module

Bluetooth module is a PCBA board which included Bluetooth functions. Bluetooth module can be used in short-distance wireless communication, which can be divided into the Bluetooth module and Bluetooth voice module according to its usage. Bluetooth module is a basic circuit set of chip which integrated Bluetooth functions and which can be used in wireless network transmission. It is a short range device of around 10 meters which provides both sound and data transmission. The Bluetooth transmits and receives at a frequency band of 2.4 GHz which is

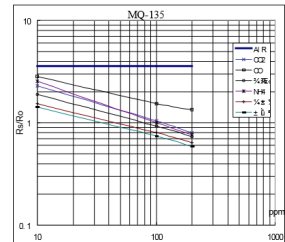
globally available. In this paper, it serves a range of about 4m to 7m.

3.4 MQ-135 Gas Sensor Module

A gas sensor is a device which detects the presence of different gases in an area, especially those gases which might be harmful to humans or animals. This sensor is used to sense the leakage of LPG (Liquefied Petroleum Gas). In normal conditions the output of this sensor HIGH and it goes LOW, when the LPG is sensed. Gas detectors can also be used to detect combustible, flammable and toxic gases, and oxygen depletion. Its detection range is 10 - 300 ppm NH₃, 10 - 1000 ppm Benzene, 10 - 300 ppm Alcohol.



(a)

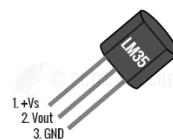


(b)

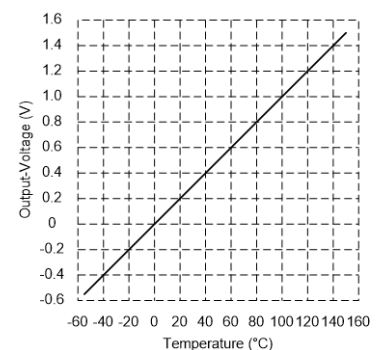
Fig 4.(a)MQ-135 Sensor Module (b) Typical Sensitivity Characteristics of MQ 135 [8]

3.5 Temperature Sensor

LM35 is a temperature sensor that is a three terminal device that provides analog voltage proportional to the temperature around it. This sensor can sense the average temperature depending on the size of room where the sensor is installed. Higher the temperature, higher is the output voltage. The output analog voltage can be converted to digital form using ADC so that a microcontroller can process it. The LM35 sensor used in this circuit can sense the operating temperature anywhere. This is ranging from -55° to 150°C. The LM35 device does not require any external calibration or trimming to provide typical accuracies of $\pm 1/4^\circ\text{C}$ at room temperature and $\pm 3/4^\circ\text{C}$ over a full -55°C to 150°C temperature range. Figure 5(b) show the Linearity of LM35(Output Voltage vs. Read Temperature)



(a)



(b)

Fig 5.(a)LM35 Temperature Sensor[8] (b) Linearity of LM35(Output Voltage vs. Read Temperature) [8]

3.6 PIR Motion Sensor

A passive infrared sensor (PIR sensor) is an electronic sensor that measures infrared (IR) light radiating

from objects in its field of view. They are commonly used in security alarms and automatic lighting applications. It detects a human being moving around within approximately 10m from the sensor. This is an average value, as the actual detection range is between 5m and 12 m.

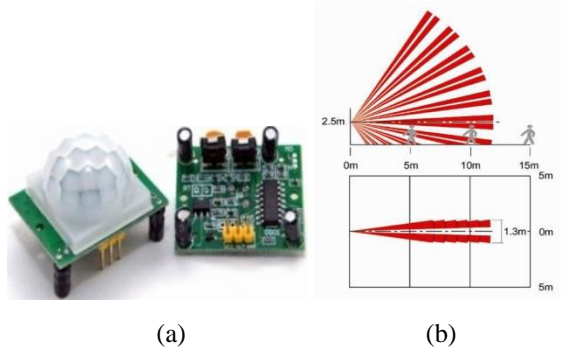


Fig 6.(a)PIR Sensor^[8] (b) Actual Detection Range of PIR^[8]

3.7 Light Dependent Resistor

A Light Dependent Resistor (LDR) is also called a photoresistor and also a photoconductor. It is basically a photocell that works on the principle of photoconductivity.



Fig 7.Light Dependent Resistor^[8]

The passive component is basically a resistor whose resistance value decreases when the intensity of light decreases. This optoelectronic device is mostly used in light varying sensor circuit, and light and dark activated switching circuits.

4. Design of Home Automation System

In this system, the operation of the system is described by two dimensions software design and hardware design.

4.1 Software Implementation of Home Automation System

The flowchart for home automation system is shown in Figure 8. The algorithm used in the flowchart is as follow.

Step 1: Start the system.

Step 2: The system is in initiation condition that all the sensors are ready to work in the same time.

Step 3: Light A, B, C, D, E (Air-con socket) and F (cook socket) can be controlled by Bluetooth and GSM via android mobile.

Step 4: If LM35 senses over 30°C then the fan starts ON else stop the fan and sensor is in initial condition.

Step 5: PIR detects motion then the street light is ON.

Step 6: LDR is in working condition, the lamp post are automatically open.

Step 7: MQ-135 senses over 70 ppm the exhaust fan starts operate and over 150 ppm sending message (Gas Alert) via GSM module.

Step 8: If the process wants to begin again, go to step 2.

TULSOJRI

Step 9: If the process wants to finish go to End.

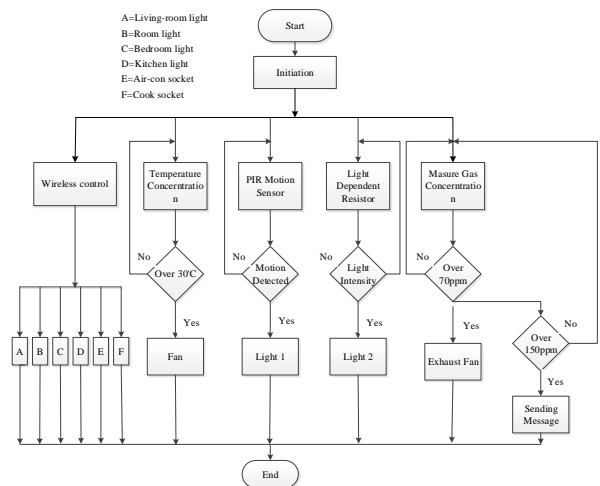


Fig 8.Flowchart of Home Automation System

4.2 Hardware Design of Home Automation System

The circuit diagram for home automation system is shown in Figure 9.

Arduino Mega is mainly used in this paper. Bluetooth Module and GSM Module are also being used. Step-down transformer is used for power supply. Four 1N4001 diodes are used as bridge to convert AC to DC. Then, voltage regulator is being used to turn down 12V to 5V from bridge diodes. 12V power supply is used for Arduino Mega 2560 through Vin pin, fan and exhaust fan. Bluetooth Module, SIM 900A and sensors are used 5V power supply. As soon as the components get supply, the system starts to operate. PIR motion sensor, temperature sensor, gas sensor and LDR are used in this system.

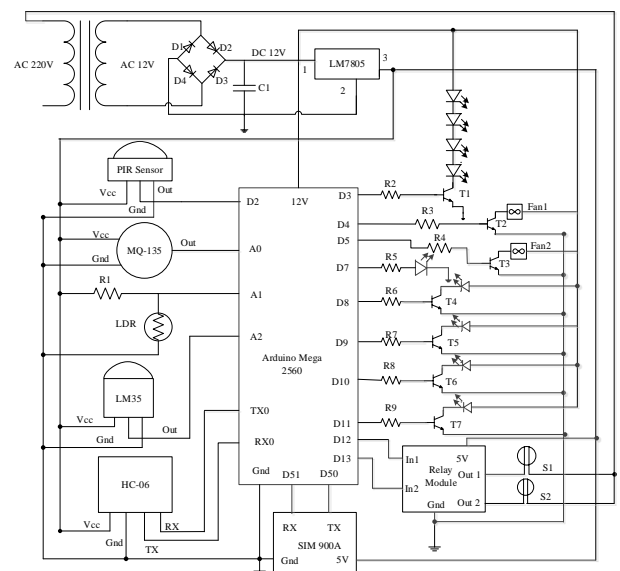


Fig 9. Circuit Diagram of Home Automation System

4.2.1 Implementation of Bluetooth Module

The transmitter (TX) pin of Bluetooth Module is connected to the Receiver (RX) pin of the Arduino Mega and the receiver (RX) pin of the Bluetooth Module is connected to the transmitter (TX) pin of the Arduino Mega.

The Arduino Mega receives AT command from the Bluetooth Module using Arduino Remote application.

```
if (terminalRead=='1')
{
digitalWrite(livingroomlight,HIGH);
Serial.println("livingroomlight on");
}
```

The user use this application to control living-room light, room light, bedroom light, kitchen room light, Air-con socket and rice cooker socket. The four outputs (living-room light, room light, bedroom light, kitchen room light, Air-con socket and rice cooker socket) are connected to the pin8, pin9, pin10, pin11, pin12 and pin13. The Bluetooth Controller application has 'ON Command' and 'Off Command'. The user can take the command as the user like and then control the appliances.

4.2.2 Implementation of Gas Sensor

The A0 output of MQ-135 is connected to the analog input pin A0 of the Arduino Mega. When the gas concentration reaches greater than and equal to 70ppm, the exhaust fan is automatically on in the kitchen. The exhaust fan is connected to the pin5 of the Arduino.

```
if (gassensor>= 70)
{
digitalWrite(exhaustfan,HIGH);
}
```

Moreover, if the gas concentration reaches over 150ppm, the mobile send SMS "Gas Alert" to the user.

```
if(gassensor>=150)
{
digitalWrite(22,HIGH);
sms.SendSMS("09256055217", "Gas Alert");
}
```

4.2.3 Implementation of Temperature Sensor

The LM35 temperature sensor is used to sense temperature in the room. The output of the temperature sensor is connected to the analog input pinA2 of the Arduino Mega. When the temperature reaches over 30°C in the room, the analog signal is sent to the Arduino and then convert analog-to-digital (ADC). Then the Arduino turn automatically ON the Fan in the room.

```
if (tempc>=30)
{
digitalWrite(fan,HIGH);
}
```

The fan is connected to the pin4 of the Arduino. 12VDC fan is used in this paper.

4.2.4 Implementation of Motion Sensor (PIR)

The passive infrared motion sensor is used for detecting motion. The sensor produces the digital output. The output pin of the PIR sensor is connected to the input digital pinD2 of the Arduino. When the PIR detects motion, the output digital signal is sent to the Arduino. Then the street light is automatically ON. The street light is connected to pin7 of the Arduino.

```
if (digitalRead(PIRinput) == HIGH)
```

```
{
digitalWrite(PIRlight, HIGH);
Serial.println("Motion detected");
}
else {
digitalWrite(PIRlight, LOW);
}
```

4.2.5 Implementation of LDR

Light dependent resistor is used for light automated ON. The output of the LDR is connected to the analog input pinA1 of the Arduino Mega. When the LDR senses intensity of light greater than 1000, the lamp post is automatically ON.

```
if(ldr_value>1000)
{
digitalWrite(ldrlight,HIGH);
}
```

4.2.6 Implementation of GSM Module

The transmitter (TX) pin and the receiver (RX) pin of GSM module are connected to the pin50 and pin51 of the Arduino Mega. If the TX and RX of the GSM module are connected right to the Arduino pin, the serial print will show "Correct DB". The Arduino Mega send AT command to the SIM 900A then it will send back "READY" to the Arduino Mega when it's connected to the mobile operator. When the SIM card is activated, the user can send AT command to the GSM Module. If the SIM card is not activated, the GSM Module could not receive the command. In this circuit, the GSM Module is used to control the air-con socket and rice cooker socket.

```
if (readString == "Con")
{
digitalWrite (cook, LOW);
}
if (readString == "Coff")
{
digitalWrite (cook, HIGH);
}
```

When the user sends "On" command, the air-con socket will be opened. If the user sends "Off" command, the air-con socket will be closed. When the user sends "Con" command, the rice cooker socket will be opened. If the user sends "Coff" command, the rice cooker socket will be closed.

5. TEST AND RESULT

The experimental results of sensors and actuators are as followed.

5.1 Testing and Result of Gas Sensor

The MQ-135 gas sensors are used in air quality control equipment. These are suitable for detecting or measuring of NH₃, NO, Alcohol, Benzene, Smoke, and CO₂. The output of gas sensor is connected to the pin A0 of the Arduino. After the user tests the gas sensor to detect gas, the LED is on as shown in Figure 10(a). When the gas concentration is greater than 150ppm, the GSM module has been sent message to the user as shown in Figure 10(b).

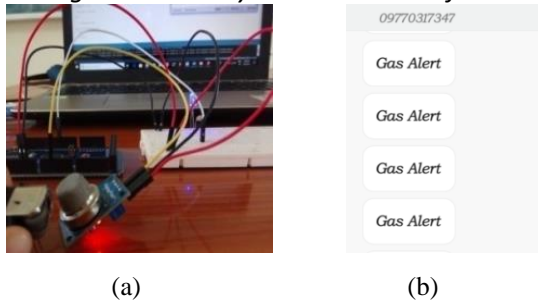


Fig 10.(a)Testing of Gas Sensor (b)Result of MQ-135 gas sensor

5.2 Testing and Result of Temperature Sensor

The temperature sensor (LM35) is used to sense temperature. The output of the temperature sensor is connected to the A2 of the Arduino. In Figure 11, the LED is shown as a result of temperature sensor.



Fig 11. Testing of Temperature Sensor

5.3 Testing and Result of PIR Sensor

PIR motion sensor is used to detect whether a human has moved in or out of the sensor range. PIR sensor activates when receives rays from any motion. By sensing these rays, it produces the output voltage. The output of the PIR motion sensor is connected to the D7 of the Arduino. In Figure 12, the LED is shown as a result of PIR motion sensor.

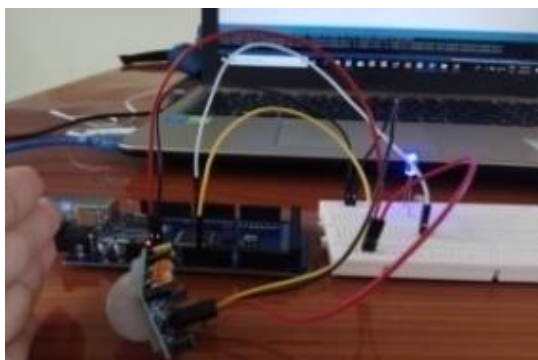
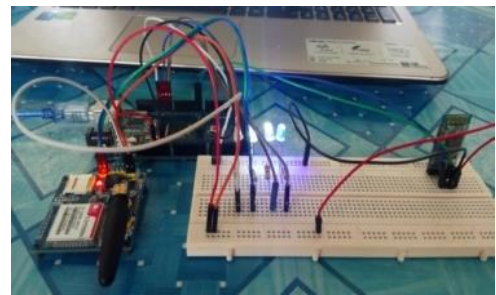


Fig 12. Testing of Motion Sensor

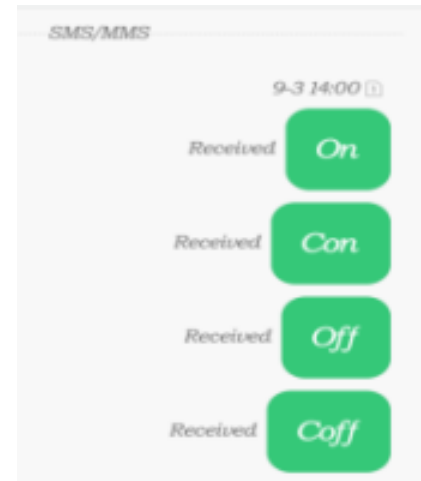
5.4 Testing and Result of GSM and Bluetooth Module

The GSM and Bluetooth Modules are connected to the Arduino Mega. The outputs are described as LEDs. The TX of Bluetooth module is connected to the RX of Arduino and the RX of Bluetooth module is connected to the TX of the Arduino. The TX and RX of GSM module are connected to the pin D50 and D51 of the Arduino. After the user send the AT commands, the four LEDs are on as

shown in Figure 13(a). The AT commands for GSM Module have been sending by the user as shown in Figure 13(b).



(a)



(b)

Fig 13.(a)Testing of GSM and Bluetooth Modules (b) Sending AT Command for GSM Module

Smart automation system has been connected as shown in Figure 14.

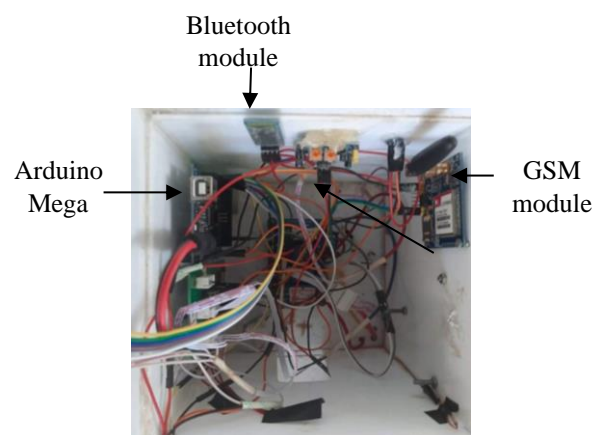


Fig 14. Connection for Home Automation System

5.5 Output Result of Home Automation System

The user can control the light of the home via bluetooth when the user is near at home or GSM when the user is far away from home. When the LM35 has sensed the set temperature, the fan is on. After PIR detected motion, the street lights are automatically on. While the LDR is in working, the lampposts are mechanically open. The MQ 135 senses the set range of the gas, the exhaust

fan start operate and senses over range the system can send the warning message to user.

6. CONCLUSIONS

In this paper, smart home automation system is proposed to easy, comfort and safe for people. Smart home automation system is a device that can perform actions and solve certain tasks without the participation of a person. The most common examples of such actions are automatic switching on and off of light, automatic correction of the heating system or air conditioner and automatic notification of fire or water leakage. Smart home automation contains a connection between wireless communication and sensors. The Bluetooth and GSM modules are used to wireless control the home appliances. The PIR motion sensor is used to detect motion and then the streetlight is automatically on when the motion detected. The LDR is also used to make the light automatically on. The temperature sensor is used to sense temperature and then to open the fan when the temperature is high. The gas sensor is used to detect and protect the gas in the home. In this case, it is not necessary to use dozens of switches when controlling lighting. In this paper the following system can be stretched. Home can be interfaced with sensors including lighting sensor and RTC (Real Time Clock). RTC can be used when the user wants to limit time for automating the home appliance. Moreover, the Arduino Mega has been leaved many pins in this thesis. So, the user can be extended in the next step. ^[4]

ACKNOWLEDGEMENT

The author would like to acknowledge the valuable criticism and comment of my Head of Department of Electronic Engineering, for her kindly advice, help, excellent guidance and permission for completion of this paper. Thanks also to the tolerant colleagues who provided all the comments and sharing their invaluable experiences to complete this paper.

REFERENCES

- [1] Yuksekkaya, B.; Kayalar, A.A.; Tosun, M.B.; Ozcan, M.K.; Alkar, A.Z.; , "A GSM, internet and speech controlled wireless interactive home automation system," Consumer Electronics, IEEE Transactions on , vol.52,no.3,pp.837- 843, Aug. 2006.
- [2] N. Sriskanthan and Tan Karande, "Bluetooth Based Home Automation Systems," Journal of Microprocessors and Microsystems, Vol. 26, pp. 281-289, 2002.
- [3] Sunny Verma, Home Automation System Using Arduino and GSM, International Research Journal of Engineering and Technology (IRJET), December 2017, <https://www.irjet.net>
- [4] Ms.PawarPallaviTatyasaheb, Home Automation System using different techniques, International Research Journal of Engineering and Technology (IRJET), June 2016, <https://www.irjet.net>

- [5] Ahmed Sirajuddin Ahmed Alhaj, Home Automation System using Arduino, Technological University Malaysia, June 2015
ahmedsirajuddin@gmail.com
- [6] RozitaTeymourzadeh, Smart GSM Based Home Automation System, UCSI University, December 2013,
<https://www.rozita@ucsiuniversity.edu.my>
- [7] <https://store.arduino.cc/usa/mega-2560-r3>
- [8] <https://www.electronicshub.org/gsm-gprs-module/>